

**LENGTH SCALE PARAMETERIZATION
AND
STABILITY ANALYSES WITH DIFFERENT
STATISTICAL METHODS IN WIND
MEASUREMENTS**

**A Thesis Submitted to
the Graduate School of Engineering and Sciences of
İzmir Institute of Technology
in Partial Fulfillment of the Requirements for the Degree of
MASTER OF SCIENCE
in Energy Engineering**

**by
Faruk TUNA**

**July 2018
İZMİR**

We approve the thesis of **Faruk TUNA**

Examining Committee Members:

Asst. Prof. Dr. Ferhat BİNGÖL
Department of Energy Systems Engineering
Izmir Institute of Technology

Asst. Prof. Dr. Hasan Engin DURAN
Department of City and Regional Planning
Izmir Institute of Technology

Assoc. Prof. Dr. Alpaslan TURGUT
Department of Mechanical Engineering
Dokuz Eylul University

04/July/2018

Asst. Prof. Dr. Ferhat BİNGÖL
Supervisor
Department of Energy Systems Engineering
Izmir Institute of Technology

Prof. Dr. Gülden GÖKÇEN
Head of the Department of
Energy Systems Engineering

Prof. Dr. Aysun SOFUOĞLU
Dean of the Graduate School of
Engineering and Sciences

ACKNOWLEDGMENTS

I would like to thank my thesis advisor Asst.Prof.Dr.Ferhat BİNGÖL for his guidance throughout this study which is a part of the NEWA project and it will be terminated in October 2018. I am very grateful to TÜBİTAK for giving me an opportunity to work in the project number 215M384 as a scholar.

I so appreciate my family for their support through my education and also it is such a great honour to be their child. Furthermore, I spent splendid times with my friends during this study which gave me positive energy to work.

ABSTRACT

LENGTH SCALE PARAMETERIZATION AND STABILITY ANALYSES WITH DIFFERENT STATISTICAL METHODS IN WIND MEASUREMENTS

When there is an attempt to find vertical wind speed and temperature profile in the absence of stability analysis then the bias is observed in those profiles. Wind profile shape can be estimated from the logarithmic wind speed formula under neutral condition since the diabatic stability term omits at that time and on the contrary, for other stability classes, this term should be derived by numerically or analytically, otherwise, the bias will be increased for wind speed and vertical temperature profiles.

In this study, the goal is to give different models and options for the masts where stability analysis can't be done by using data where comes from conventional masts. Here, different 2 kinds scenarios will be given to see better:

Scenario 1: No stability analysis applied. Conventional mast measurements are used where the wind speed measurements are at two different heights, the temperature is from only one location, and wind direction measurements are from wind vanes. Therefore, unwanted occasions occur such as overestimate and underestimate for unstable and stable conditions, respectively.

Scenario 2: Stability analysis applied by using the sonic anemometer which provides high-frequency data and vertical wind velocity. After determining diabatic wind term, wind speed can be corrected by implementing diabatic term into profile equation.

As a summary, those two scenarios are compared and in order to get correct measurements different models for the conventional masts are given.

ÖZET

RÜZGAR ÖLÇÜMLERİNDE FARKLI İSTATİSTİKİ METOTLARLA YÜZEY KATMANI DERECELENDİRMESİ VE KARARSIZLIK ANALİZİ

Stabilite analizi yokluğunda dikey rüzgar hızı veya sıcaklık profili bulma girişimi olduğunda bu profillerde yanılmalar görülür. Rüzgar profili normal koşullar altında diabatik terim olmadığı için logaritmik rüzgar hızı formülü ile bulunabilir ve bunun aksine kararlı ya da kararsız durumlarda nümerik veya analitik olarak elde edilir. Yoksa dikey rüzgar hızı ve sıcaklık profillerinde yanılmalar olacaktır.

Bu çalışmada ana amaç geleneksel ölçüm cihazlarından gelen datalarla stabilite analizinin yapılmadığı yerlerde kullanılabilecek farklı modeller ve seçenekler sunmaktır. Burada, daha iyi anlamak için 2 farklı senaryo verilecektir:

Senaryo 1: Kararsızlık analizi yok. 2 farklı yükseklikten rüzgar hızı ölçümü yapıldığı, sıcaklığın ise tek bir noktadan alındığı, ve rüzgar yönlerinin rüzgar güllerinden alındığı geleneksel ölçüm direkleri kullanılmaktadır. Bu yüzden, kararsız ve kararlı durumlar için sırasına göre abartılı ya da olması gerekenden az hesaplanması gibi istenmeyen durumlar meydana gelmektedir.

Senaryo 2: Yüksek frekanslı ve dikey hız ölçümlerini sağlayan sonik anemometreler kullanılarak kararsızlık analizi yapılabilir. Diabatik hız terimi elde edildikten sonra profil denklemleri içine koyularak rüzgar hızında düzeltmeler yapılır.

Sonuç olarak bu 2 senaryo kıyaslanmakta ve doğru ölçümler elde etmek için geleneksel direkler için farklı modeller verilmektedir.

TABLE OF CONTENTS

LIST OF FIGURES	viii
LIST OF TABLES	ix
CHAPTER 1. INTRODUCTION	1
1.1. Literature Survey	1
CHAPTER 2. WIND MEASUREMENT TECHNIQUES	7
2.1. Conventional Measurement Techniques.....	8
2.2. New Generation Remote Sensing Devices	10
2.2.1. Sodar	11
2.2.2. Lidar	12
CHAPTER 3. ATMOSPHERIC BOUNDARY LAYER AND WIND CHARAC- TERISTICS	13
3.1. Logarithmic Wind Profile	19
3.2. Atmospheric Stability	23
3.2.1. Monin-Obukhov Similarity Theory	25
3.2.2. Mixed Layer Similarity	28
3.2.3. Local Similarity / z-Less Stratification	29
3.2.4. Local Free Convection Similarity	29
3.2.5. Rossby Number Similarity.....	30
CHAPTER 4. STABILITY ANALYSIS IN COMPLEX TERRAIN	31
4.1. Test Equipment and Setup	32
4.2. Measurement Campaign	38
4.3. Data Analysis	39
4.3.1. Flux-Profile Relation	41
4.3.2. Richardson Method	42
4.3.3. Wind Shear Exponent	44
CHAPTER 5. RESULTS	46

CHAPTER 6. DISCUSSION	52
CHAPTER 7. CONCLUSION	53
REFERENCES	54

LIST OF FIGURES

<u>Figure</u>	<u>Page</u>
Figure 3.1. Diurnal changes of the atmospheric boundary layer	14
Figure 3.2. Comparison of dominant forces in the ABL	18
Figure 3.3. Logarithmic wind profile	20
Figure 3.4. Aerodynamic roughness lengths and terrain types. Source:Stull (2012); Hicks et al. (1975); Garratt (1977); Nappo (1977); Smedman- Höngström & Höngström (1978); Thompson (1978); Kondo and Ya- mazawa (1986)	22
Figure 4.1. Time and spatial scales of wind flow	31
Figure 4.2. IZTECH meteorological mast	34
Figure 4.3. Technical drawing of the IZTECH meteorological mast and equip- ments	34
Figure 4.4. Instruments are mounted on the IZTECH met mast, starting from the a to the l, sensor names and their locations are given, too.	35
Figure 4.5. Technical drawing of the booms for the top and backup anemometers at 101 and 99 m, respectively, and wind vane at 98 m. Top anemometer, wind vane and backup anemometer are represented by a), b), and c), respectively.	36
Figure 4.6. Technical drawing of the booms for the sonic anemometers and tem- perature/humidity sensors. Sonic anemometers mounted at 52 m and 10 m, while temperature/humidity sensors mounted at 3-35-90 m.	37
Figure 4.7. Location of the IZTECH met mast	38
Figure 5.1. Dimensionless Obukhov length parameters for the stable region at 10 m	46
Figure 5.2. Dimensionless Obukhov length parameters for the stable region at 52 m	47
Figure 5.3. Dimensionless Obukhov length parameters for the unstable region at 10 m	48
Figure 5.4. Dimensionless Obukhov length parameters for the unstable region at 52 m	49
Figure 5.5. Comparison of stability classes by MOST and wind shear exponent	50
Figure 5.6. Wind velocities at different heights from met mast	50
Figure 5.7. Normalized wind velocity versus height graph	51

LIST OF TABLES

<u>Table</u>		<u>Page</u>
Table 4.1.	IZTECH 100 m met mast properties	39
Table 4.2.	Derived parameters	39
Table 4.3.	F-P Relationships for instability cases by Businger et al.	41
Table 4.4.	F-P Relationships for instability cases by Dyer	42
Table 4.5.	F-P Relationships for instability cases by Zilitinkevich and Chalikov ...	42
Table 4.6.	Stability classes with the shear exponent	45

CHAPTER 1

INTRODUCTION

As it is known, to calculate friction velocity, momentum and heat fluxes, is not possible by using conventional methods since 3D measurements (u,v,w components) and temperature measurements at different heights are needed. However, approaches such as Richardson method, wind shear parameter, and flux profile relations can be used in the absence of the given measurements. When the data collected from the conventional sensors are used in the wind energy researches, wind flow analyses software, it will be bias in the results since the collected data are not reliable.

To overcome the problem several models can be used is discussed. In upcoming chapter, firstly a literature survey is given about the history of the boundary layer meteorology, right after the related topics with this study and conventional in-situ sensors are discussed. In next chapter all the theories related with the atmospheric boundary layer will be given and it should be noted that to scale is a very crucial step since the validation of the theories only belongs to that region. In chapter 4, stability analyses will be given with different ways. A comparison among them and limitations for applying to data are also given. Results of the measurements, derived values, and analyses are given at Chapter 5, deficient of the study and future work is given at Chapter 6 and conclusions are given at Chapter 7.

1.1. Literature Survey

Latest studies of atmospheric boundary layer goes way back to 1850s, starting with the research of Reynolds (1883), Taylor (1935), Taylor (1938), and Prandtl (1925). Reynold stresses used in obtaining covariance of parameters. Taylor put forward the frozen term in turbulence. Prandtl has put forward the logarithmic wind profile theory in which stated that mixing length is proportional to the height above the earth surface and shear stress is constant in the SL. Basically, the velocity profile has given as:

$$u_z = const \times \log(z/z_0) \quad (1.1)$$

where z_0 is integration constant and const term is called as Von Karman con-

stant denoted by κ . Sutton, 1931 modified the eddy diffusivity that was studied by L. F. Richardson and G. I. Taylor in the same era but in addition to them Sutton has suggested a new diffusion coefficient which is constant for the large areas. In Sutton's work it was stated that after sufficient time the final motion of eddies are not resemble to the initial motion since the source of eddies get weaker by time or by the distance enough and in the end, initial motion is influenced by the large eddies which is the new source of the motion. In his work, effective eddy distance defined for near the ground and very high altitudes. As result, his work is valid for even up to 600 km and depending on the observation period diffusion effects vary.

Halstead (1943) derived a stability term in addition to Prandtl's work by using the data from Thornthwalte and Kaser. When that term is to put into logarithmic wind velocity equation, vertical velocity profile turns into:

$$u(z) = \frac{(\tau/\rho)^{1/2}}{k_0} \ln(z/z_0) + \left(\frac{c\alpha_p}{T_0} \right) (z - z_0) \quad (1.2)$$

Here the last term at the right-hand side is the stability term. The results of Halstead's work give a comparison between the logarithmic and instability cases.

By using Prandtl's and Richardson's works, Holzman (1943) derived a mixing length by considering the stability effects and lapse rate. In his work mixing length height is given for both stable and unstable stratification like:

Unstable:

$$l_s = \frac{l}{\sqrt{1 + \beta \frac{g}{T} \left(\frac{\partial T}{\partial z} + \Gamma \right) / \left(\frac{\partial u}{\partial z} \right)^2}} \quad (1.3)$$

and

Stable

$$l_s = l \sqrt{1 - \beta \frac{g}{T} \left(\frac{\partial T}{\partial z} + \Gamma \right) / \left(\frac{\partial u}{\partial z} \right)^2} \quad (1.4)$$

where lapse rate denoted by Γ , velocity gradient denoted by $\partial u/\partial z$, and β is the proportionality factor. In additionally if the case is neutral mixing length becomes 0 since the denominator goes to infinity. He also showed that the influence of evaporation on the stability problem and he derived evaporation equation which defined as:

$$E = \frac{\rho k_0^2 (q_1 - q_2)(u_2 - u_1)}{\ln\left(\frac{z_2}{z_1}\right)} \left[\frac{1}{\ln\left(\frac{z_2(1-sz_1)}{z_1(1-sz_2)}\right)} \right] \quad (1.5)$$

here, s is related with the buoyant force and also includes wind gradient and temperature gradient terms, q represents humidity and k_0 comes from logarithmic expression, and u is the velocity. As s goes to 0, evaporation occurs under the adiabatic/neutral conditions.

Lettau (1950) has studied on the Leipzig wind profile which comes from Mildner's work (1931) and seen that even small changes in the azimuth angle are enough to make influence the geostrophic wind.

Many types of research about the surface layer have done during the 1950s when many of the Soviet researchers have worked about SL since it was important for agrometeorology and geophysics.

Since then, field experiments have been prepared and these experiments required for the use of sensors to observe the characteristics of the ABL.

In the first decade of the 20th century hot-wire anemometers have been used to study developed turbulence in the atmosphere. Kaimal and Finnigan (1994), state that this type of sensors are known as in situ sensors that can be mounted on the ground, on masts, towers, balloons, or aircraft. Cup and sonic anemometers which have been improved rapidly are also part of the in situ sensors. Monin and Obukhov (1954) have analyzed the process of mixing flow in turbulent atmosphere and proposed a method to compute wind velocity and temperature gradients.

Panofsky et al. (1960) worked on the diabatic wind profile. They compared their observation with the theoretic results of Ellison (1957), which it is inferred that theoretic results agree well with the observation when the similarity class is near neutral and unstable. Another conclusion of their work is that log-linear approach doesn't work well under instability.

Blackadar (1962) investigated the geostrophic wind. He assumed that the K_m coefficient is dependent to dissipation energy as $K_m \propto \epsilon^{1/3}$. His findings work well at surface layer when the turbulence eddies are independent of height. Basically his work is important aspect of showing the vertical distribution of wind and exchange coefficients.

Wyngaard et al. (1971) have evaluate expressions for Reynolds shear stress and heat flux. Their work also include local free convection conditions of ABL where MOST doesn't work. Results such as heat and momentum fluxes and wind shear have been studied for extreme unstable conditions.

Dyer and Hicks (1970) have put forward relation between dimensionless parameters such as momentum, heat, and moisture coefficients and ζ where the limit is between 0.01 and 1, which affects the coherence between theoretic relation and observation.

Businger et al. (1971) have shown relations between dimensionless parameter like Richardson number, momentum, heat coefficients, eddy transfer ratio (α), and ζ in which they took several different interval for the experiment such as 30 min, 45 min, and 1 h.

Businger et al. (1971) analyzed wind and temperature profiles for a wide range of stability condition by using MOST and they managed to compute Richardson number from the profiles and their results between profile-measured and derived were in good agreement. Different approaches for ϕ_m , ϕ_h have been considered for $\kappa = 0.40$ and $\kappa = 0.40$ where the difference is seen in ϕ_h more than ϕ_m . Besides, Ri and α , Ri and κ , and the relations between momentum and heat parameters also given.

Golder (1972) have showed the effect of surface roughness on the dimensionless parameters such as L, Ri, and Ri_B . Pasquill and Turner categories has used in their work as a classification system. The most important result here is to see the direct relation between surface roughness and Obukhov length.

Dyer (1974) published a review of flux profile relations have been studied until that time. Those are for both stable and stable regions where they are all assumed as 1 for neutral conditions.

Foken and Skeib (1983) have summarized flux profile relations like Dyer (1974) but with the difference where they used new data from the MESP-81 Tsimtyansk experiment.

Schotanus et al. (1983) have investigated the accuracy and availability on the temperature measurements by sonic anemometer since the humidity affects virtual temperature much more as it gets higher. They suggest 2 methods to find heat flux, which they are using Bowen ratio and using net radiation.

Kot and Song (1998) improved classic approach in which basically vertical eddy fluxes used to estimate ζ and they have showed the difference of thermal roughness length or heat transfer roughness length with their expression. Parameters those are used in their model are ζ , z/z_0 , and z/z_T . Their results also showed that improved model of their can be used for any kind of surface and for a wide range of instability.

Byun (1990) has studied on the analytical solutions of F-P relations which is hard to obtain. He suggested some solutions for both stable and unstable conditions where those solutions are valid for extreme conditions. Surface fluxes, exchange coefficients can be found after finding the Ri number.

Grachev et al. (2000) revisited the Kansas-type formulae where convective form also included. Their intention was to fit constant for the empirical relations of F-P relations and they found different values under certain circumstances.

Yang et al. (2001) have suggested an analytical solution which is used for the stable conditions and they used thermal surface roughness instead of aerodynamic surface roughness since they used surface radiometric temperature. For stable layer their approach comes from the idea which is using the linear profile relation, while they have only managed to give approximate solution for unstable region.

Gryning et al. (2007) have did analyses by using data from 160 m mast at Høvsøre and 205 m TV tower at Hamburg for the aim of to obtain better relation which is wanted to represent of entire vertical layer reaching the top. Basically, they derived relations for middle and upper part and have put an expression that gives better scaling of vertical structure. The inverse of mixing length is inverse summation of surface, middle, and upper boundary layer lengths. Surface layer height reaches to 50-80 m

Grachev et al. (2007) have analysed SHEEBA (Surface Heat Budget of the Arctic Ocean Experiment) data sets where mostly stable stratifications occur. They investigated profile relations under extreme stable conditions such as free convection and strongly stable conditions. Their results contain Ri number and profile relations, Ri_B and ζ , deviation of wind speed with increasing wind, and they also derived profile functions and diabatic term for SHEEBA case.

Sorbjan and Grachev (2010) haven't only studied on the data from SHEEBA but also they considered the data from the CASES-99 (Cooperative Atmosphere Surface Exchange Study 1999). Stable stratification has been divided 4 categories in their works such as "nearly neutral", "weakly stable", "very stable", and "extremely stable" conditions where they considered local fluxes instead of surface fluxes. As a result they also found that Pr number is 0.9 in near neutral conditions and it is 0.7 in the very stable conditions.

Floors et al. (2013) have included wind lidar into the study of the wind prediction models and boundary layer analyses which is up to 800 m. They used cup, ultrasonic, and lidar measurements with different scenarios. In their WRF model they used YSU (Yonsei University) and MYNN (Mellor Yamada Nakanishi Niino) boundary layer models.

Jiménez et al. (2012) have studied WRF model for surface layer which includes flux profile relations. They also have improved relation between Richardson number and profile parameters with dimensionless Obukhov length. Their new formulae take part in fixing the unwanted part of the distributions of parameters such as friction velocity, wind

speed, and temperature which is similar to high pass filter where the fluxes values become extreme and results become unclear in the absence of it.

Dias et al. (2012) have presented a vehicle in order to measure temperature and humidity with high resolution which is very important for vertical scaling. They have calculated heat flux and spectra of the measurement which the time series of the measurements are not long enough.

Peña and Hahmann (2012) have compared difference methods such as ζ Ri_B number, WRF, sonic fluxes, and long term stability. Their result indicate good agreement among for all the methods when necessary filtering and exclusion is done.

Burns et al. (2012) have also studied on the sensible heat fluxes since there is direct relation between humidity and temperature. In the area where their experiments are performed there is forest on the surface. They have found that the wind speed affects heat flux measurements, too which is at maximum when wind speed is 18 m/s.

Grachev et al. (2013) have studied on the limits of MOST for stable stratification of air. They also interest with the critical Ri number which gives idea turbulence and found inequality between flux and gradient Ri number. When both flux and critic value of Ri is between 0.20 and 0.25 turbulence scales are getting small but may not be disappear. They also studied on the local z-less stratification and have shown the spectra effect on the profile parameters.

Arnqvist et al. (2015) have studied on forested area where located at Ryningsnäss in Sweden with the 138 m tall tower. They have tried to evaluate errors and uncertainty in wind measurements to get better data quality. It is interesting result that eventhough being invalid, surface layer approaches have follow the theoretical curves where it reaches to the 100 m. Besides, the other result is that aerodynamic roughness length has effect on the instability such as it increases 50 % from stable to the neutral conditions.

Dellwik and Jensen (2005) have worked on the forested area, internal boundary layer, and profile scaling functions such as momentum and heat. It can be found in their study that the aerodynamic resistance vary less for sensible heat flux respect to the momentum flux. Furthermore, relations for the displacement height and aerodynamic roughness those are depending on the mean wind speed have also been given.

In the last decade mostly remote sensing as lidar and sodar measurements have gained importance to be used in stability analyses.

CHAPTER 2

WIND MEASUREMENT TECHNIQUES

Measurement is a basically a number or a quantity which are investigated or wanted to know. Therefore, it is needed to be known how to measure those numbers and to understand what they indicate. There are some important terms about measurements which they are directly related with previous sentence, that is to say these terms actually give meanings to numbers (Landberg, Lars 2016):

-*Representative*: Serving as a portrayal or symbol of something.

-*Resolution*: The smallest interval measurable by a scientific instrument.

-*Accuracy*: The degree to which the result of a measurement, calculation or specification conforms to the correct value or a standard. Bias and scatter are the terms have been contained by accuracy which means how much measurements are accurate that is what the bias and scatter of data display. In mathematically bias related with mean and scatter related with standard deviation.

-*Precision*: Refinement in a measurement, calculation or specification, especially as represented by the number of digits given.

To know how much those numbers are reliable, one should investigate the data respect to terms above and should also include recovery rate which tells whether the measurement is sufficient enough or not and to say enough, it should be higher than 0.9 respect to many sources in literature. It is defined as (Landberg, 2015):

$$R = \frac{\text{Number of valid data points}}{\text{Number of possible data points}} \quad (2.1)$$

After knowing the meaning of those numbers one should also know how to get them. Measurements are come from field or wind tunnel and numerical simulations (Stull, 1988). Sensors are the device to measure and mostly providing a continuously varying output and an analogue to digital encoder samples output as discrete digital record (Stull, 1988). There are also some additional instruments such as platform for instruments, display devices and so on.

Sensors are used to collect data which represents the characteristics of the ABL. Depending on the perspective they can split many categories, but only two types of the definition have given here. For the location of sensors where they have mounted, they

have divided categories such as conventional and remote sensing. Conventional sensors are also called as in situ sensors. On the other hand, according to their sampling rate (frequency) sensors have divided into two categories which those are fast-response and mean value sensors.

2.1. Conventional Measurement Techniques

In situ sensors are used for measuring at the location where the sensors are mounted. They can be located at ground, balloons, tower and etc. In situ sensors generally used for near ground and they measure mean and fluctuation. In order to contain all the turbulent effects the necessary accuracy for in situ sensors are basically $\pm 0.05 m/s$ for wind velocity, $\pm 0.05^\circ C$ for temperature and $\pm 0.05 mb$ for pressure. Furthermore for the fluctuation sensors the response time shouldn't be achieve 0.1 s (Kaimal and Finnigan, 1994).

There are some advantages and disadvantages of the conventional sensors. The sensitivity, the accuracy and the simplicity are the advantages of the in situ sensors. While modification of the flow is big handicap for these sensors since they measure at the location where they are getting effected from distortion of flow (Stull, 1988).

For profile measurements required sensors are listed below (Stull,1988; Kaimal and Finnigan, 1994; Landberg,2016):

Wind Velocity

Cup anemometers are generally used for obtaining wind velocity and the most used type is three cup anemometer and the logic behind it is, drag against cups causes rotation and that gives a voltage which can be translated to wind speed. However those don't give fast response measurements and for that reason sonic, gill, hot wire, gust vane, pitot, aspirator, drag sphere, pivot arm, pibal that is nothing but pilot balloon tracked by theodolite or radar, venturi, and rotometer where fluid moving vertically in conical tube lifts a ball in tube are used to get .

To get accurate wind measurements cup and other sensors should be calibrated. For this reason wind tunnel are used for calibrating this devices but since the steady flow rarely occurs in atmosphere. The better approach is that using in situ calibration technique in which sensors are wanted to be calibrated are to put up near the ones with known properties. There is a linear relation between wind speed and rotation of cup which is defined as:

$$U = AX + B \tag{2.2}$$

where X is the rotation and A and B are coefficients, and U is wind velocity. This coefficients are to be found after calibration. In order to get more information about cup and other sensors check the (Kaimal and Finnigan,1994; Landsberg, 2016; Stull, 1988)

Wind Direction

Wind Vane and bivane used where vanes point in direction where wind comes from while bivanes pivot up/down as well as left-right to give elevation angle and compass direction.

Temperature Measurements

Temperature is the first kick to start motion in the boundary layer in atmosphere. So its dynamics have to be known. Sensors generally take measurements from different heights cause what is needed to be known is vertical gradient of temperature. Mostly sensors have $\pm 0.05^\circ C$ accuracy and $\pm 0.01^\circ C$ resolution according to (Kaimal and Finnigan, 1994). Fast response sensors for the temperature measurements are thermocouples, thermistors, hot wires, and sonic anemometers/thermometers, while the mean value sensors are liquid in glass, wax thermostats, bimetallic strips, and quartz crystals.

Sonic anemometers are to be investigated more. As a start the logic behind them using sound as doppler shifting principle. There are heads positioned as they are looking at each other and a signal transmitted from one of them to the opposite one. The propagation time is the key to get wind velocity since the distance between heads and the speed of sound are known. Time delay is the first step and after that wind velocity is to be find by using it in Equation 2.3

$$\begin{aligned} t_1 &= \frac{L}{C + V} \\ t_2 &= \frac{L}{C - V} \end{aligned} \tag{2.3}$$

Next step is to get wind velocity after organizing Equation 2.3 which yields to Equation 2.4

$$\begin{aligned} U &= \frac{L}{2} \left(\frac{1}{t_1} - \frac{1}{t_2} \right) \\ C &= \frac{L}{2} \left(\frac{1}{t_1} + \frac{1}{t_2} \right) \end{aligned} \tag{2.4}$$

Humidity

Most known sensors are psychrometer, hair hygrometer, chilled mirror, hygistor

for mean measurements and Lyman-alpha and IR hygrometers, and microwave refractometer for fast response measurement (Stull,1988).

According to many work in literature humidity is not easy to measure and there are many definitions for it such as; vapour pressure, absolute humidity and relative humidity.

Pressure

Mercury in glass gives mean pressure measurements and aneroid and capacitive elements give fast response records. Both of the aneroid and capacitive type of barometers are very classic equipment and thanks to developments on the electronics and semiconductors technology there are digital type of the barometers (Landberg, 2016 and Stull,1988).

Radiation

Most known sensors are:

Radiometer and net radiometer are where the total radiation and only difference between bottom and top of a hemisphere taken into consideration, respectively. Other sensors are pyranometer, pyrliometer, diffusometer and prygeometer and these are also use similar theory for measuring radiation with radiometers.

2.2. New Generation Remote Sensing Devices

Remote sensors are separated two categories active and passive respect to logic behind them. That is to say, when a sensor generates its own wave such as light, sound or microwave, and it comes back to that sensor these are named as active remote sensors. While passive ones only have the receiver part and gets wave from other sources such as sun, earth or the atmosphere (Stull, 1988).

Disadvantages of remote sensors are their size, the more complexity, the more inability to measure boundary layer characteristics, since they are signal problems for manipulating and filtering them i.e. there are noise to get rid of them. On the contrary, advantages of remote sensors are the mobility to use many area, their fast to scan an area, a line of the the atmosphere where it starts propagated from ground (Stull, 1988).

Which sensors are used to obtain which atmospheric variable will be addressed first and then more information about Sodar and Lidar will be given.

Wind Velocity and Direction

Doppler radar, doppler sodar, doppler lidar, and lidar are used. Its principle is basically using microwaves, sound, and light. The doppler shift effect is the idea of to get wind velocity. Doppler shift is defined as:

$$\Delta f = \frac{\Delta v}{c} f_0 \quad (2.5)$$

where Δf is the change of emitted frequency, f_0 and received one by sensors, Δv is the velocity difference between emitter and receiver, c is the speed of light/sound/microwave.

Temperature

Microwave sounders, lidar, mirages are used to get mean velocity measurements, and scintillation, radiometers, and sodar give fast response measurements.

Humidity

Lidar and radar are used to measure humidity. The principle is aerosol swells in humid air in lidar and variations in refractive index in radar systems.

For RS there is no directly measurements are taken, it can be obtain by using governing equation where other parameters such as velocity and temperature comes with wave propagation (Stull, 1988).

2.2.1. Sodar

Sodar gets mean sound detection and ranging and this type of sensors probe atmosphere by using sound propagation. This devices are ground based instrument and transmit a sequence of short burst of sound waves at audible frequencies 2000-4000 Hz upward in three different directions into the atmosphere (Peña et al., 2015).

After 2005, there are some improvements about signal processing and that makes the performance better. Additionally, there is another type of Sodar which known as Doppler-RASS (radio acoustic sounding system) which is used for estimating mixing layer height. And the working principle is that as a key parameter virtual temperature are measured directly by using RASS. Basically it becomes sodar and additional instruments such as electro-magnetic emitter and receiver where the doppler shift effect used again to estimate radiation caused by sound waves, and the propagation speed of sound is defined as following (Peña et al., 2015):

$$c_a = -\frac{0.5c\Delta f_e}{2f_{e,0}} \quad (2.6)$$

where operating frequency is $f_{e,0}$, the doppler shift is Δf_e , and speed of light is c . For more information about this system one can go and check (Peña et al., 2015) and can

see that there are many other sort of RASS system used, too.

2.2.2. Lidar

The meaning of Lidar is light detection and ranging system and the logic behind is that again using the doppler shift effect and tracking the backscatter of the light caused by a laser with a well defined wavelength about $1.5 \mu m$ and even the small shift of frequency can be detect in the weak backscattered light.

In Lidars, 2 type of beam are used which they are continuous and pulsed beam in which beams are transmitted from ground to different directions or heights, therefore, measurements from different heights and directions can be obtain at the same time. Another advantage of ground based systems that avoiding the turbulence effects as in met-masts.

Firstly, continuous wave lidars is to be given. The beam of laser transmits continuously and measures in same way, receives backscattering again, continuously. In order to get measurement at different heights lens are used in a way that for short distance bigger lens are used. Several lidar are used in energy market and most known ones are ZephIR, WINDAR which are as told earlier, CW type of lidar.

Second and other type of beam used lidar is pulsed lidar and this one transmits a sequence of many short pulses, and mostly 30 m in effective distance and sure the doppler effect is the physic behind the scene where backscattered light waves gives reason it. Contrary to CW lidars, in here, there is no dependence to measuring distance. The most known ones in the market are Wind-Cube, Wind tracer, Vindicator, and Galion.

As a comparison it can be state that CW lidars are give data in perspective of better resolution near short distance, they are better for turbulence measurements, and they can give wind speed measurements up to 150-200 m as a vector and radial speed, respectively. On the contrary pulsed lidars are at constant resolution and slower than CW lidars but advantage of pulsed ones they can give measurements at more than one height simultaneously. Last improvements about lidars are that becoming more mobile and more realistic, besides in the near future it is expected that they can be fully integrated with turbine control systems which makes more productive and long term systems (Peña et al., 2015).

CHAPTER 3

ATMOSPHERIC BOUNDARY LAYER AND WIND CHARACTERISTICS

Structure of atmospheric boundary layer is basically composing of different layers such as surface layer where we live, Ekman layer, and free atmosphere in perspective of Wind Meteorology. However, as it can go complicated different types of classification systems can be seen for meteorology science which they are Troposphere, Stratosphere, Mesosphere, Thermosphere, and there are transition zones in the between of the layers as Tropopause, Stratopause, and Mesopause, respectively. The thickness of surface layer differs from 50 m to 200 m in diurnal cycle, Ekman Layer starts from surface layer and reaches to 1000-1500 m, and then free atmosphere starts. Both of the SL and EL form the planetary boundary layer and theories and formulas are to be given are only valid of in this region for Wind Meteorology. In order to make it short different regions from atmospheric boundary layer denoted as (Stull,1988):

BL : Ekman Layer

BL : Boundary Layer

CL : Cloud Layer

FA : Free Atmosphere

IBL : Internal Boundary Layer

ML : Mixed Layer

RL : Residual Layer

SBL : Stable Boundary Layer

SCL : Sub-cloud Layer

SL : Surface Layer

In Figure 3.1, it can be seen that there are many changes in diurnal cycle in which it starts with sunrise that gives reason an increment at potential temperature caused by

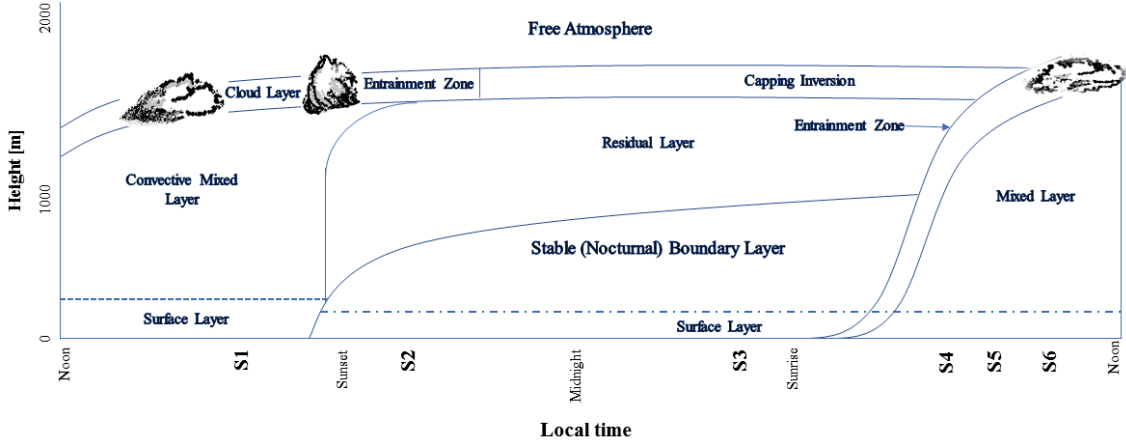


Figure 3.1. Diurnal changes of the atmospheric boundary layer
(Source:Stull 2012)

sun which makes the boundary layer thicker. Afternoon BL becomes more convectively driven and it starts to sink with sunset therefore, residual layer occurs caused by the difference of stable (Nocturnal) BL and top of the ML. The heights of the layers in the atmospheric boundary layer shown as h , z_i , z_r , and z_b which they are heights of the SBL, RL, and top of the sub-cloud layer. The ABL depth can be found by using expression suggested by Sutton (1953) which obtained from geostrophic balance and defined as (Kaimal and Finnigan, 1994):

$$z_h = \pi \left(\frac{2K_m}{f} \right)^{0.5} \quad (3.1)$$

where K_m is the momentum exchange coefficient, f is the Coriolis parameter which will be defined in the Equation 3.18. After realizing that K_m is not constant with height then another assumption has been accepted which suggested by Tennekes 1952 and reveals that depth of ABL is proportional to $\frac{u_*}{f}$, where u_* is friction velocity near the ground and another approach for boundary layer depth:

$$z_h = C \frac{u_*}{f} \quad (3.2)$$

here, C is a coefficient and estimated as 0.25 empirically. Even being a better approximation it is also not reliable since the frictional and Coriolis effects suppressed by the external forces, e.g. lapse rate, subsidence inversion.

Von Karman (1930), suggested that since the nature of wind is logarithmic;

$$l = \frac{-ks}{ds/dz} \quad (3.3)$$

Here, s is the magnitude of the wind shear and k is Von Karman constant. This approach is valid for surface layer and it is similar with Prandtl (1932);

$$l = kz \quad (3.4)$$

here, λ represents the free atmosphere length scale and according to Bernstein (1959) for special conditions such as neutral condition, one meter roughness and 10m/s geostrophic wind speed it is:

$$\lambda = 0.00027G/f \quad (3.5)$$

In 1962, Blackadar suggested new expression for length scale;

$$\frac{1}{l} = \frac{1}{\kappa z} + \frac{1}{l_0} \quad (3.6)$$

In this equation as a new parameter l_0 seems and it indicates characteristics of eddies and it is a scale of energy. In order to find l_0 Brost and Wyngaard suggested a model and here it is assumed that inertia and buoyancy forces are in a balance and $l_0 = l_B$;

$$l_B = C \frac{\sigma_w}{N} \quad (3.7)$$

N is the Brunt-Väisälä frequency, σ_w is characteristic velocity scale and C is constant which is 1.69 suggested by Brost-Wyngaard. In order to find σ_w one should look at the variance of vertical turbulent velocity and for determining N ;

$$N = \left(\frac{g}{T_0} \frac{\partial \Theta}{\partial z} \right)^{1/2} \quad (3.8)$$

In Blackadar and Delage (1986), they suggested for determining characteristic length for turbulent length scale.

$$\frac{1}{l_i} = \frac{1}{(0.64/f_i)z + (0.17/f_i)\Lambda} \quad (3.9)$$

In this equation, i represents three components of vector and for each component f_i changes. According to Sorbjan case study (1986), for $i=x,y,z$ f_i values are 0.33, 0.058 and 0.22, respectively.

Zilitinkevich and Baklanov (2002) has suggested a formula for determining atmospheric boundary layer that;

$$z_i = 0.1 \frac{u_{*0}}{f} \quad (3.10)$$

Gryning et al. (2007) derived a new model by considering the all ABL which is;

$$\frac{1}{l} = \frac{1}{l_{SL}} + \frac{1}{\kappa l_{MBL}} + \frac{1}{l_{UBL}} \quad (3.11)$$

Where the UBL and MBL indicate upper and middle part of the ABL and SL indicates surface layer.

$$l_{UBL} = \kappa(z_i - z) \quad (3.12)$$

and for middle boundary layer it has determined as;

$$l_{MBL} = \frac{u_{*0}}{f \left(-2 \ln \left(\frac{u_{*0}}{fz_0} + 55 \right) \right)} \exp \left(\frac{\left(\frac{u_{*0}}{fL} \right)^2}{400} \right) \quad (3.13)$$

Peña et al. (2010) have suggested a formula which is;

$$\frac{1}{l} = \frac{1}{\kappa z} + \frac{(\kappa z)^{d-1}}{\eta^d} \quad (3.14)$$

Here, η indicates the maximum length scale and d is the control parameter for controlling the growth of the scale. For d parameter, Blackadar (1962), Lettau (1962) and Peña et al. (2010) have suggested 1, 5/4 and 5/4, respectively. Both value can be used. The maximum length scale parameter is shown as;

$$\eta = \frac{\kappa z_i}{d(1+d)^{1/d}} \left[\left(\left[\ln \left(\frac{u_{*0}}{f_c z_0} \right) - A \right]^2 + B^2 \right)^{1/2} + \ln \left(\frac{z_i}{z_0} \right) \right]^{-1/d} \quad (3.15)$$

A and B parameters are empirical and change respect to stability cases and these values are given in Peña et al. (2010).

Equations from 3.3 to 3.15 are different approaches have been done where Monin-Obukhov length scale theory has not been putted there since it will be given under the atmospheric stability.

As a definition it can be say that wind is motion of air. Therefore, there are several forces which give reason to this motion. The driven force is pressure gradient but the change of diurnal air temperature is the main reason behind the scene. Air temperature gets higher with sunrise and air molecules energy is, too, density of the molecules decrease. Afterwhile, they start to rise and the more getting higher the more temperature decrement occurs. That means pressure increases and air parcels flow from high pressure to the low pressure locations. In order to get an idea about wind flow which forces give reason this phenomenon need to be known. Those are (Landberg, 2016):

-frictional force

$$\vec{F} = -a\vec{U} \quad (3.16)$$

a is a constant depends on surface characteristics and \vec{U} is wind velocity as a vector.

-gravitational force

$$\vec{F}^* = G \frac{m_1 m_2}{r^2} \frac{\vec{r}}{r} \quad (3.17)$$

here, m_1 and m_2 are masses, G is the universal gravitation constant, r and \vec{r} are the distance and vector form of the distance, respectively. It is very known formula which is the Universal Gravitation Law of Newton, since the masses are small here, this force generally is to be neglected.

-Coriolis force

$$\vec{C} = -f \vec{k} \times \vec{U} \quad (3.18)$$

f is the Coriolis parameter which is $2\Omega\sin\phi$ where ϕ is latitude and Ω is the speed of Earth ($7.29210^{-5}rad/s$), and \vec{k} is the unit vector that pointing in the the direction of the rotation vector.

-pressure gradient

$$\vec{P} = -\frac{1}{\rho}\vec{\nabla}P \quad (3.19)$$

as it can be seen here, pressure force comes from gradient of pressure which denoted as $\vec{\nabla}P$, and ρ is the density of air parcel.

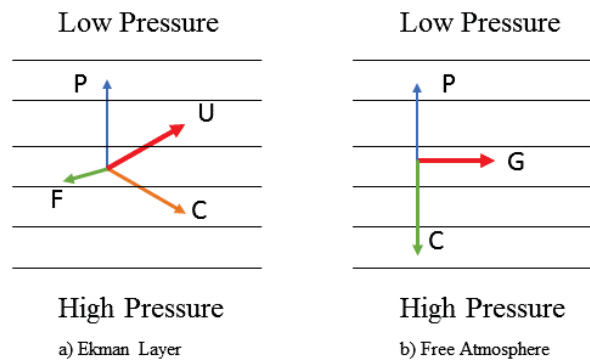


Figure 3.2. Comparison of dominant forces in the ABL
(Source: Landberg 2015)

Therefore, wind is an airflow which becomes from reasons as it is placed above and a wind can be separated into 3 categories:

-Mean Wind:

This flow dominates horizontal movements of air or in other saying is transporting of air which is very fast in BL and responsible from advection of pollutants in the atmosphere. Mean wind gradient as defined before is maximum near the ground since frictional forces. It is known that vertical mean speed are so small respect to horizontal mean wind speed and order of mm or cm per second (Stull,1988).

-Waves:

Waves generally occurs at night times and affects transportation of scalars such as humidity, heat, pollutant, even explosions and thunderstorms, and so on. They occurs from the reason that the mean wind shear and flow over an obstacle.

-Turbulence:

Under surface layer viscous forces are effective and therefore turbulence occurs here, however, above boundary layer turbulence can be seen in convective clouds, and near the jet stream which they create clear air turbulence (CAT) since there is high wind shear. Turbulences in the boundary layer are irregular motions of air, which becomes from forces acting on the ground or from thermals. The motion takes swirls form and the small ones feeds bigger ones. The largest eddies in the boundary layer are seen from 100 m to 3000 m and they are a way more than effective from molecular diffusivity at transporting quantities like scalars or pollutants.

Air motion is spatial and time dependent function and in order to observe this motion, measurements are taken at a one location over a time period instead of trying to observe a large domain at an instant time since the former option is much more easier than last one. There is a simplification on considering turbulence revealed by G.I. Taylor who suggested that turbulence may thought as frozen. In order to do this simplification it is necessary that the time scale for turbulent eddies should be longer than the time necessary for eddies to advect to the sensor which revealed by (Powell and Elderkin, 1974). Following equation tells what is the meaning of frozen word and defined as:

$$\frac{dC}{dt} = 0 \quad (3.20)$$

C is any variable and total derivation of C is zero and total derivation is becomes as $d()/dt = \partial()/\partial t + V_i \partial_i()$ where V_i indicates the velocity components by index notations. Therefore Equation 3.20 yields to

$$\frac{\partial C}{\partial t} = -U \frac{\partial C}{\partial x} - V \frac{\partial C}{\partial y} - W \frac{\partial C}{\partial z} \quad (3.21)$$

Another showing way of this theory in perspective of wave number is:

$$\kappa[\text{rad/m}] = \frac{f[\text{rad/s}]}{M[\text{m/s}]} \quad (3.22)$$

where κ is $2\pi/\lambda$ and f is $2\pi/P$ where P is period and λ is wavelength suggested by Wyngaard and Clifford, 1977. Another suggested approach is made by Willis and Deardorff, 1976 which implies that standard deviation of velocity should fulfill a condition in order to be valid, that is $\sigma_M = 0.5M$

3.1. Logarithmic Wind Profile

The definition of wind profile is related with the wind velocity and altitude from the ground. So, depending on the definition one can state that logarithmic wind profile is log-shape profile where velocity changes with log-function of the height. Typically, it can be shown as:

$$u(z) = \frac{u_*}{\kappa} \log \left(\frac{z}{z_0} \right) \quad (3.23)$$

As it can be seen from here, logarithmic wind profile depends on parameters such as friction velocity, Von Karman constant, and roughness length. This is actually very old formula which came from Prandtl's works. Simply, when there is a flow over a surface, the velocity gradient is maximum at the surface, and it is nearly 0 far from the ground. It can be seen easily in Figure 3.3

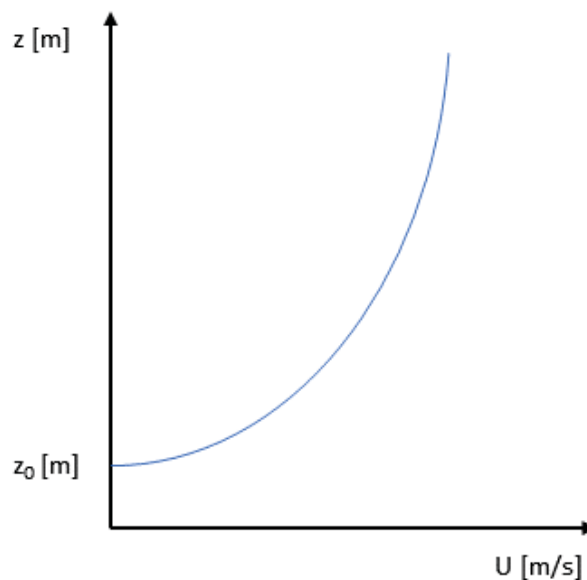


Figure 3.3. Logarithmic wind profile

Wind gradient gets bigger above the roughness length while wind velocity is zero under this length. Besides roughness length can't be estimated easily. Many approaches have been done to obtain this parameter and still going on (Smedman-Högström & Högström, 1978; Hicks, et al, 1975; Garratt, 1977; Nappo, 1977; Thompson, 1978; Kondo and Yamazawa, 1986).

In order to comment whether air is neutral or not temperature gradient is the way to get answer. If potential temperature gradient is zero, it is obvious that air parcels are neutral, i.e. there is no motion upward or downward in that altitude. The rate of change of temperature with height called as lapse rate and these two terms are different but dependent each other. Potential temperature is defined as

$$\frac{\partial \theta}{\partial z} = \left(\frac{\partial T}{\partial z} + \frac{g}{c_P} \right) \quad (3.24)$$

where $\theta = T \left(\frac{P_0}{P} \right)^{R/c_P}$, P is the pressure at height where the measurements are taken, c_P is the specific heat of dry air and it is $1004 J/kgK$, R is the gas constant which is $287 J/kgK$ for dry air. There is another term called as virtual potential temperature and defined as

$$\theta_V \equiv \left(\frac{\theta}{T} \right) T_V \quad (3.25)$$

where $T_V = T(1 + 0.61r)$ for unsaturated air and $T_V = T(1 + 0.61r_{sat} - r_L)$ for saturated air. Here, T is the dry air temperature at the location which is interested, r is the water-vapour saturating mixing ratio of unsaturated air parcels while r_{sat} and r_L are saturated water-vapour and liquid-water mixing ratio of saturated air parcels. And, T_V is the temperature where dry air and moist air have same density at same pressure.

As it is known from earlier, thermals are one of the driven forces in the atmospheric layer and warm air starts to raise since density of air parcel smaller than surrounding air. On the contrary, when surrounding air has temperature higher than the air parcel then air parcel sinks. Virtual temperature is the parameter used to determine the denouement of the vertical motion of air parcels in the ABL (Stull, 1988).

There is also another concept which is known as aerodynamic roughness which should be estimated from at least 2 height and so the value of roughness near the ground will differ from the aerodynamic roughness which also depends another altitude. There is one important thing for this 2 parameter, which, once the aerodynamic roughness parameter estimated for a particular surface, it doesn't change with wind velocity, stability class or stress, it changes when the roughness near ground changes that is caused by the effect of height and coverage of vegetation, obstacles such as houses, fences and forests (Stull, 1988). For estimating aerodynamic roughness length some methods have been suggested:

Charnock (1955), his approach was used for estimating sea surface which defined as;

$$z_0 = \frac{\alpha_C u_*^2}{g} \quad (3.26)$$

but Chamberlain (1983) showed that it gives good result for blowing sand and blowing snow roughness depend on α_C coefficient and it can be see in Figure 3.4

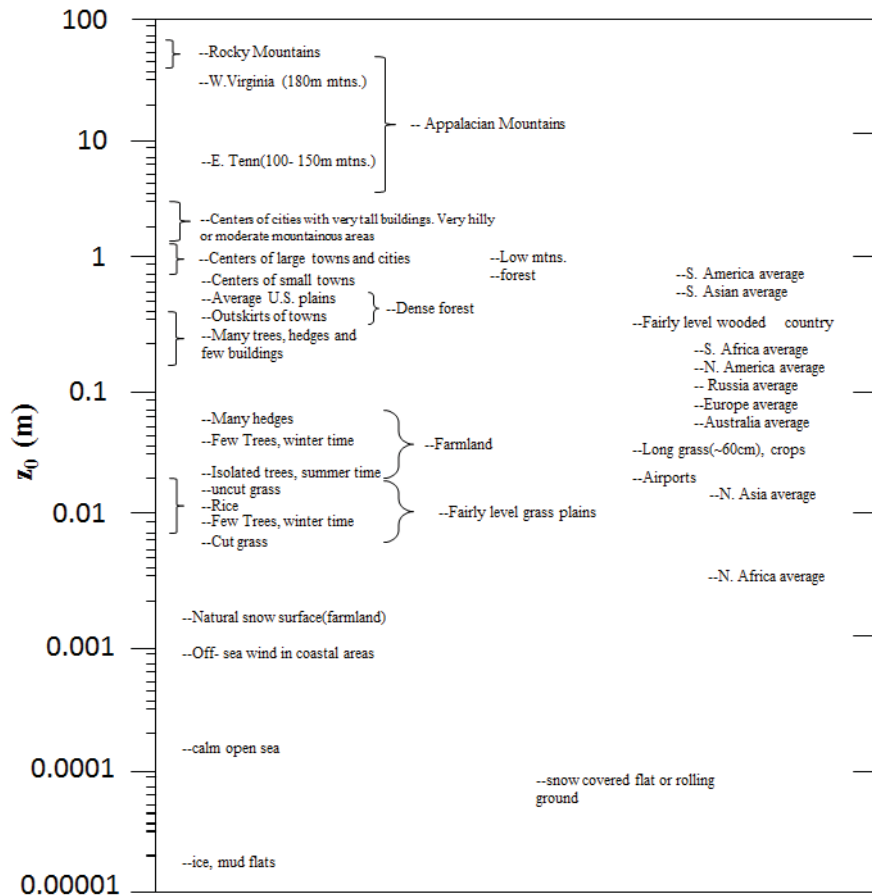


Figure 3.4. Aerodynamic roughness lengths and terrain types. Source:Stull (2012); Hicks et al. (1975); Garratt (1977); Nappo (1977); Smedman-Höngström & Höngström (1978); Thompson (1978); Kondo and Yamazawa (1986)

In Figure 3.4, surface roughness values are given for many different type of surfaces. As it can be seen from there it is minimum at ice and sea surfaces and maximum at forest and mountains.

For Lettau (1969), this approach suggested formula for estimating z_0 which is defined as

$$z_0 = 0.5h^* \frac{s_S}{S_L} \quad (3.27)$$

In Lettau's approach, h^* is averaged vertical extent of the roughness elements, s_S is averaged vertical cross section area of one element and S_L is lot size per element where S_L is total ground surface area / number of elements . For this approach, there are some restrictions such as roughness elements shouldn't be close to each other and they should have similar geometries (Stull, 1988).

Kondo and Yamazawa (1986), their approaches work well for buildings and cities where buildings in city are taken consideration as elements for their model. Important parameters are surface area and height of those elements since the model uses both of them for each individual elements.

$$z_0 = \frac{0.25}{S_T} \sum_{i=1}^N h_i s_i \quad (3.28)$$

3.2. Atmospheric Stability

Stability is a term that indicates the tendency of the air whether air flow goes upward or downward and this motion makes atmospheric phenomena like precipitation or affects cases like propagation of pollutants or any scalars. There are two kind of air stability concepts such as static and dynamic.

Static air stability is related with thermals and buoyancy is the driven force here. When less dense air lies under the more dense one this creates a motion and since it is not caused by wind static terms used for it. The motion caused by inequality of density makes unstable case and air parcel underlies the more dense air parcel starts to go upward until reaching the balance. The unstable air eventually becomes turbulent or if it is already turbulent it will remain turbulent, while stable air becomes or remain laminar. But of course, there can be change between this 2 cases since there are many factors or driven force those can be affect air flow in the atmosphere (Stull, 1988).

Dynamic stability indicates that there is a motion of air and not only thermals but also wind flow is driven force, too. If the flow is driven by wind or in other word if it is act like forced flow then more dense air can flow underlie less dense air where wind shear and the stable stratification occur (Stull, 1988). In order to understand this case better Thorpe (1969)-(1973), Woods (1969) have been carried out experiment where they used

2 different fluids such as water and dyed brine in laboratory. They have put forward the behaviour of the flow as:

- As initial condition there is wind shear at the interface

- When the critical value of wind shear achieved (critical Richardson number) it turns to unstable flow and waves starts to form

- After growing enough those waves start to *roll up* or *break* which calling as Kelvin-Helmholtz wave, and the physic behind this event is different than the waves at the ocean.

- When the waves roll both of the less denser and more denser fluids included by the waves and less denser one result as static instability. This situation is also called as *cat's eye* or *breaking wave* patterns.

- Static and dynamic instability combine with each other and turbulent occurs.

- The result of spread turbulence on the layer is that a mixing of fluids or a diffusion process between the fluids where fluxes such as momentum, heat, and moisture are transferred between them. This process eventually yields to a unclear, much broader, and more diffuse shear layer where the shear effects are weaker and static stability occurs.

- The mixing process may also reduce the shear below the critical value and dynamic instability can be eliminated.

- As the shear effects are not supported by continuously turbulence gets weaker at the interface and flow gets back to original position to put it in different way flow become laminar again.

It is related with the last sequence that in the presence of the high and continuous wind shear gradient such as nocturnal jets and strong wind jets turbulence can go on for hours to days which called as **CAT**. According to findings this flow can effect large horizontal areas reaching to hundreds of kilometers.

It is known that respect to Newton's 3rd law of motion for every action there is an equal opposite reaction. When instability occurs it gives reason for a reaction force such as turbulence for dynamically unstable air flow and convection for statically unstable air flow. To understand much better Richardson number gives idea about the situation of air(Stull,1988).

As it is stated earlier ABL becomes several layer and in order to know this layers height scaling is a crucial tool and there are several classes of similarity scales in the literature till now which they are basically define as:

Monin-Obukhov Similarity:

Mixed-Layer Similarity:

Local Free Convection:

Rossby Number Similarity:

All of this similarity scales are valid in the range where they are defined.

3.2.1. Monin-Obukhov Similarity Theory

MOST is valid in surface layer where the Coriolis force can be neglected and dynamic velocity which is nothing but momentum flux that can be assumed as constant. Monin and Obukhov, 1954 shows that this layer is thin and limit reaches to the 50 m. This theory have been used by many authors such as Wyngaard, 1973; Sorbjan, 1986 and it is also known as *constant flux layer* since the fluxes such as heat, moisture, and momentum vary less than 10% of their values with height. In addition, MOST has another restriction that in order to work well winds shouldn't be calm and u_* should be different than 0 or it can be state that instead of mesoscale effects turbulent effects are needed.

Rate of changes of relevant scale values in the SL are given here (Stull, 1988):

L : Order(1 m to 200 m)

z_0 : Order(1 mm to 1 m)

u_* : Order(0.05 to 0.3 m/s)

θ_*^{SL} : Order(0.1 to 2°C)

q_*^{SL} : Order(0.1 to 5 g_{water}/kg_{air})

In this layer most important parameters are momentum, heat, and humidity fluxes and their definitions are following (Kaimal and Finnigan, 1994):

$$\tau = K_m \rho \frac{\partial \bar{u}}{\partial \bar{z}} \quad (3.29)$$

$$H = -K_h \rho c_p \frac{\partial \bar{\theta}}{\partial \bar{z}} \quad (3.30)$$

$$E = -K_q \rho \frac{\partial \bar{q}}{\partial \bar{z}} \quad (3.31)$$

where $K_m, K_h,$ and K_q are the turbulent exchange coefficients for momentum, heat, and moisture. This expression is belong the K-theory and eddy covariance can also be used for estimating SL parameters. For this reason, taken measurements are decomposed into their means and fluctuations parts:

$$u = \bar{u} + u'$$

$$v = \bar{v} + v'$$

$$w = \bar{w} + w'$$

$$\theta = \bar{\theta} + \theta'$$

$$q = \bar{q} + q'$$

there is an important rule by definition $\bar{u}' = \bar{v}' = \bar{w}' = \bar{q}' = \bar{\theta}' = 0$ and lets the mean wind flow only x direction then means of the other component at y and z direction becomes 0 and only \bar{u} differs from the 0 and fluxes in the SL can be expressed as:

$$\tau = -\rho \overline{u'w'} \quad (3.32)$$

$$H = \rho c_P \overline{w'\theta'} \quad (3.33)$$

$$E = \rho \overline{w'q'} \quad (3.34)$$

MOST theory uses basically 3 parameters as buoyancy, kinematic flux, and heat flux at the surface. Here, $E/\rho = \text{constant}$ since it belongs the SL. Scaling parameters of the SL is to express by using them. Scaled velocity and temperature are given as:

$$u_* = \left[-(\overline{u'w'})_0 \right]^{0.5} \quad (3.35)$$

$$T_* = \frac{-(\overline{\kappa w'\theta'})_0}{u_*} \quad (3.36)$$

This 2 parameters is used for obtaining Obukhov length at surface or near the surface and it is given as:

$$L = -\frac{u_*^3}{\kappa \left(\frac{g}{T_0} \right) \left(\frac{H}{\rho c_P} \right)} \quad (3.37)$$

where $H/\rho c_P = \overline{w'\theta'} = \text{constant}$, g/T_0 is the buoyancy, and u_* is the friction velocity at the surface. Besides all of these the reason of using Obukhov length scale is make clear of the situation of air which is basically:

-Stable Condition : $L > 0$; heat flux $(\overline{w'\theta'})$ is negative which means air parcel tends to go downward.

-Neutral Condition : $L \rightarrow \infty$; $(\overline{w'\theta'})$ goes to 0 and air parcel stands still at that place.

-Unstable Condition : $L < 0$; heat flux is positive and air parcel goes upward.

Instead of Obukhov length scale most of the time it can be seen that dimensionless Obukhov length scale is chosen in order to show stability classes, which is defined as $\zeta = z/L$; and here z is the altitude where the measurements are taken.

It has expressed that in the logarithmic wind profile wind velocity given as only dependent on the surface roughness, friction velocity, and Von Karman constant. However, after using MOST theory and finding the stability classes it differs from the logarithmic profile as the stability class is not in the range of neutral condition. A.S. Monin found a way that to add a term which is known as stability term or diabatic wind term into logarithmic wind velocity equation to obtain better wind measurements and following equation it can be seen.

$$u(z) = \frac{u_*}{\kappa} \left[\ln \left(\frac{z}{z_0} \right) - \psi \left(\frac{z}{L} \right) \right] \quad (3.38)$$

Diabatic term denoted as ψ and seems that it is function of the dimensionless stability length scale and it comes from the integration of the velocity profile function (Peña, 2009):

$$\psi_m = \int_0^{\zeta} \frac{1 - \phi_m(\xi)}{\xi} d\xi \quad (3.39)$$

where ϕ_m is the velocity profile function, and for

neutral conditions:

$$\phi_m = 1 \text{ and } \psi_m = 0;$$

stable conditions:

$$\psi_m = -b_1 \frac{z}{L};$$

unstable conditions:

$$\psi_m = 2 \ln \left(\frac{1+x}{2} \right) + \ln \left(\frac{1+x^2}{2} \right) - 2 \arctan(x) + \frac{\pi}{2}; p_1 = -1/4$$

$$\psi_m = 3/2 \ln \left(\frac{1+x+x^2}{3} \right) - \sqrt{3} \arctan \left(\frac{2x+1}{\sqrt{3}} \right) + \frac{\pi}{\sqrt{3}}; p_1 = -1/3$$

where $x = \left(1 - a_1 \frac{z}{L} \right)^{-p_1}$ and for p_1 different 2 values has suggested by Stull (2012) and Gryning et al. (2007), respectively. In the Flux-Profile Relation section this term will be given much more comprehensively. Other parameters like a_1 and b_1 will be given under this section, too, since different values suggested by the authors depending on the case study.

3.2.2. Mixed Layer Similarity

In this layer fluxes are not constant and that is the reason for MOST is not works here. Top of this layer changes diurnal and scales of fluxes and lengths are given as Stull (2012)

z_i : Order of 0.2 to 2 km

w_* : Order of 2 m/s

θ_*^{ML} : Order of 0.1 K

q_*^{ML} : Order of 0.1 g/m³

u_* : Order of 0.02 m/s

In this layer fluxes are expressed depending on K-theory which is defined as Arya (1984) :

$$\overline{u'w'} = -K_m \frac{\partial \bar{u}}{\partial z} \quad (3.40)$$

$$\overline{v'w'} = -K_m \frac{\partial \bar{v}}{\partial z} \quad (3.41)$$

$$\overline{\theta'w'} = -K_H \frac{\partial \bar{\theta}}{\partial z} \quad (3.42)$$

$$\overline{q'w'} = -K_E \frac{\partial \bar{q}}{\partial z} \quad (3.43)$$

where these K values are momentum, heat, and humidity exchange coefficients and prescribed as $K_m = K_H = K_E \approx 0.15\lambda_{mw}\sigma_w$. Here, λ_{mw} and σ_w are length and velocity scales which they are given in Appendix C and

There are another manipulation on the velocity exchange coefficient which is (Prandtl, 1931):

$$K_m = l^2 \frac{\partial U}{\partial z} \quad (3.44)$$

where $U = \sqrt{\left(\frac{\partial u}{\partial z}\right)^2 + \left(\frac{\partial v}{\partial z}\right)^2}$ and it is known that far from the ground this relation does not work well (Prandtl, 1925), (Sutton, 1932). As it is given in literature source is the origin of the turbulence and momentum exchange coefficient can be found near the source. Sutton (1932) has shown that far from the source, mesoscale becomes dominant force.

3.2.3. Local Similarity / z-Less Stratification

The reason for calling z-Less is that depending on the height is getting less important in this layer Wyngaard and Coté (1972); and Wyngaard (1973) and there is another important concept, too, which is surface fluxes are lost their importance and local fluxes get much more important those are momentum, heat, and humidity. Limits of the scales are Stull (1988):

L_Λ :Order of 0 to 50 m

u_Λ :Order of 0 to 0.3 m/s

θ_Λ :Order of 0 to 2.0 °C

q_Λ :Order of 0 to 5 $\text{g}_{\text{water}}/\text{kg}_{\text{air}}$

Profile parameters are function of only ζ in this layer and given as Garratt (1992):

$$\begin{aligned} \phi_m &= C_m \zeta \\ \phi_h &= C_h \zeta \end{aligned} \quad (3.45)$$

here, C_m is easy to get but on the other hand C_h is related with ζ and Pr number (Monin and Yaglom, 1971).

3.2.4. Local Free Convection Similarity

In this region MOST doesn't work since mean wind speed are seemed and that makes ζ so close to 0 and z (local height) is used instead of z_i . This situation occurs under condition such as static instability and turbulence existence at the surface layer. The scales of the parameters are following (Stull, 1988):

z :Order of 0 to 50 [m]

w_{LF} :Order of 0 to 0.5 [m/s]

θ_{LF} :Order of 0 to 2 [°C]

q_{LF} :Order of 0 to 5 [g_{water} / kg_{air}]

Depending on the findings of Wyngaard et al. (1971), friction velocity doesn't change with large ζ values and the region of this layer is between $[L, z_i]$.

3.2.5. Rossby Number Similarity

In this region both are taken into account since it is wanted to put a relation between surface effects and top of the layer, therefore relevant parameters are either surface and free atmosphere parameters. There is dimensionless number defined by using geostrophic wind and surface roughness and frequency by Tennekes (1984) which is called as Rossby number and found as:

$$Ro = \frac{G}{f_c z_0} \quad (3.46)$$

The relations between velocity and height scale is given by following equations for top of the boundary layer and surface layer, respectively:

$$\bar{U} - U_2 = \frac{u_*}{\kappa} f \left(\frac{z}{h_2}, \frac{h_2}{L} \right) \quad (3.47)$$

$$\bar{U} = \frac{u_*}{\kappa} \left[\ln \left(\frac{h_2}{z_0} \right) + \psi_m \left(\frac{z}{L} \right) \right] \quad (3.48)$$

Equation 3.47 is valid for above the middle atmospheric layer and Equation 3.48 is near the ground, the relation between top of the BL and SL can be obtain from this relation.

CHAPTER 4

STABILITY ANALYSIS IN COMPLEX TERRAIN

Complex terrain may be defined as anywhere out of the flat terrain that's mean definition directly related with the surface roughness. Changing terrain, hills, and plant canopies are good examples, however, complex terrain actually represents steeper where surface roughness characteristic very effective on the flow.

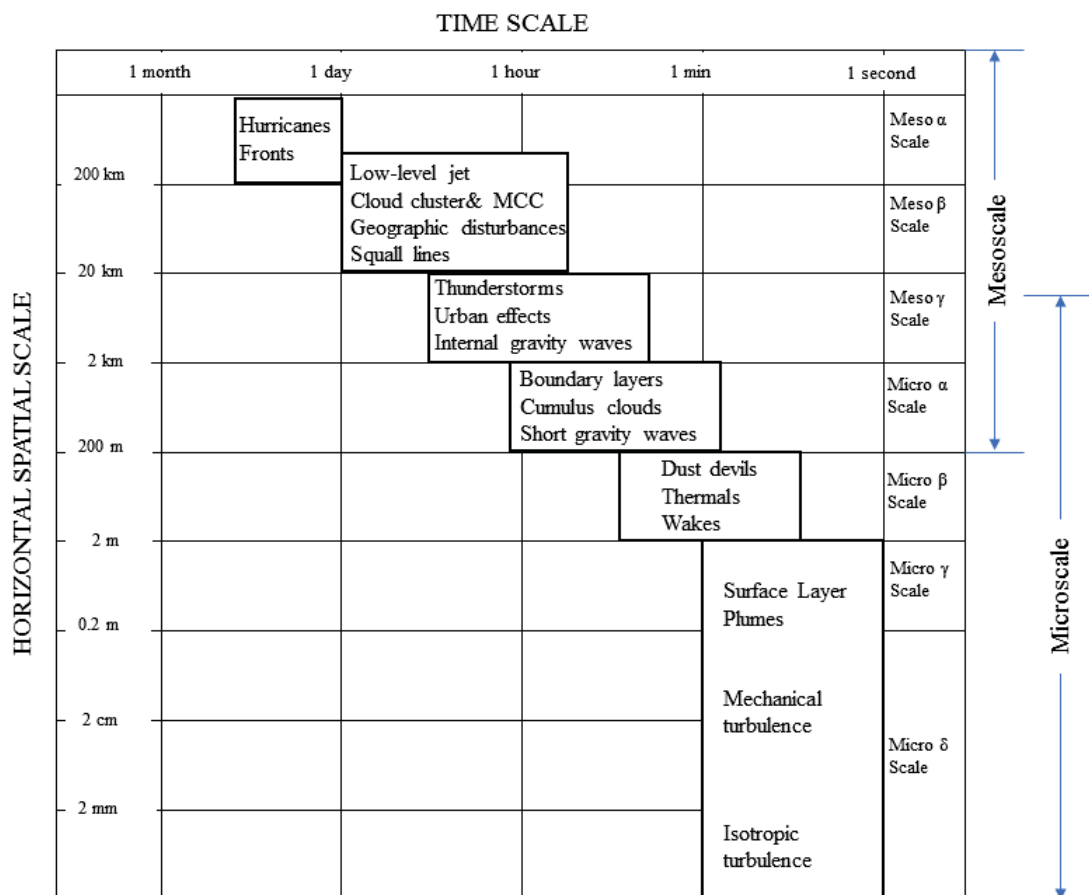


Figure 4.1. Time and spatial scales of wind flow
(Source: Stull 2012)

In Figure 4.1 microscale and mesoscale can be infer for both time and spatial scale. For the sake of this study best range of time interval is 10 min. It is important to know that this interval may not be enough to observe turbulence effect so that shorter

periods may be used to get rid of this problem.

Mostly theories such as Richardson, F-P are not work well over the complex terrain however it is possible to improve the qualities of those approaches by putting the surface parameter into them as in (Panofsky et al., 1982). Turbulence mostly occurs by mechanical effects like changing surface roughness, flow over steeper hills, or flow over the interface between the sea and land surfaces.

4.1. Test Equipment and Setup

The IZTECH meteorological mast has established after finding the location which is the pre-work for this study and it took for 5 months to select a location. There were three options to choose the place of the met mast and the second best option has chosen for some special reasons. However, current location is better in terms that not only stability but also turbulence may be studied since the region is complex terrain. Before mounting all the equipments it is very important to check up for stability of mast to be sure it is not shaking that caused by loose ropes. Next work is the mounting all the equipments such as sensors, cables, data loggers, and etc. A picture from IZTECH met-mast can be seen in Figure 4.2 and as a standard IEC 61400-12 applied on during the setup.

In order to understand better it is necessary to look for technical drawing of the met mast. It can be seen in Figure 4.3, while mounted instruments are seen in Figure 4.3. The height of the met mast is 101 m where instruments are settled as one lightning rod and cup anemometer placed at the top, flash light mounted at 93 m, 3 wind vane putted at 98-74-28 m, backup and other anemometers mounted at 99-76-30 m, humidity and temperature sensors were located at 3-35-90 m. These are the instruments of the met-mast.

Vectorial quantities such as velocity and direction are taken from anemometers and wind vanes. On the other hand, scalar parameters like moisture and temperature are taken from the sensors shown in Figure 4.4. Top anemometer and backup anemometer are given in a) and b), and wind vanes are given in d), e), and f) where they are mounted at discrete heights.

In Figure 4.4, g) represents the ultrasonic 3D anemometer mounted at 52 m, h) used for other sonic anemometer mounted at 10 m, temperature/ humidity sensors those located at 3-35-90 m has shown in i), air pressure sensor at 2 m has shown in j), solar panel has shown in k), and aviation light lastly shown in l) which used for prevent the met mast from any accident. These are the instruments set-up on the mast.

The boom geometries and technical drawing of the instruments are given in Figure 4.5 and Figure 4.6. In Figure 4.5, a) represents the geometries of the boom geometries of the cup anemometer at 101 m, boom geometries of the wind vane at 98 m has shown in b), and c) represents the boom for the cup anemometer at 99 m.

Boom geometries of cup anemometers are given in Figure 4.5, too. In part a) boom dimensions for cup anemometer at top given where the dimensions of that instrument are very different rest of the components. In part b) boom dimensions of the wind vane mounted at 98 m have shown, and c) represents the boom for the cup anemometer which mounted at 99 m and it is known as the backup anemometer since when the top anemometer takes damage, it is used to measure. In d) boom dimensions for the wind vanes mounted at 74 m and 28 m given, while e) represents the dimensions of the cup anemometers mounted at 76 m and 30 m. As it can be seen the dimensions are same for b) and c), while the instruments are different. There is same situation for d) and e). On the other hand depending on the height different dimensions for the same sensors applied. That difference occurs by the reason of ground effect which is mostly the surface roughness.

In Figure 4.6 booms for the sonic anemometers and temperature/humidity sensors are given. Here the distance of the boom from the mast and sensors height can be seen. Sonic height is higher than the temperature/humidity sensors. Since wind velocity can be affected easily from the vibration extra cautions are taken as it can be seen from the picture.

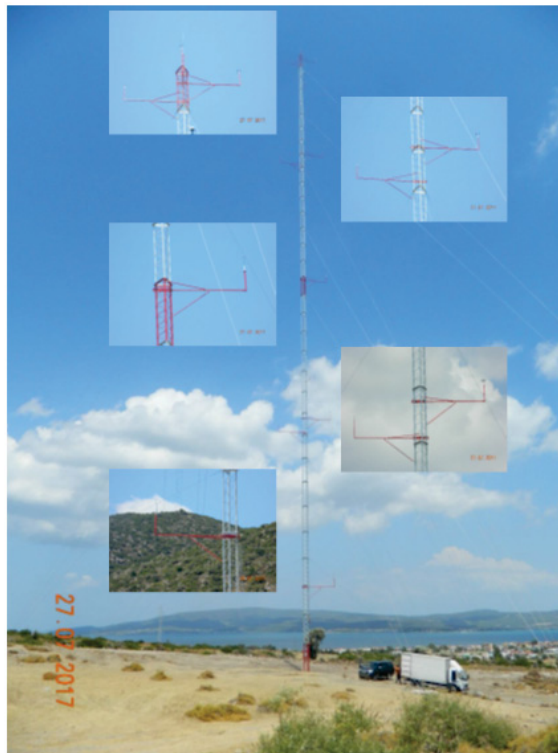


Figure 4.2. IZTECH meteorological mast

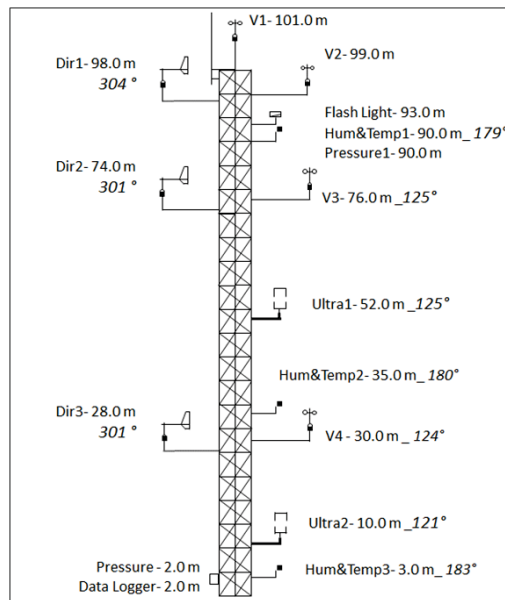


Figure 4.3. Technical drawing of the IZTECH meteorological mast and equipments



a) Top anemometer



b) Backup anemometer



c) Reference anemometer



d) Wind vane I



e) Wind vane II



f) Wind vane III



g) Ultrasonic 3D Anemometer (@10m)



h) Ultrasonic 3D Anemometer (@52m)



i) Temperature/ Humidity Sensor @3m, 35m, and 90m



j) Air Pressure Sensor (@2m)



k) Solar Panel



l) Aviation light

Figure 4.4. Instruments are mounted on the IZTECH met mast, starting from the a to the l, sensor names and their locations are given, too.

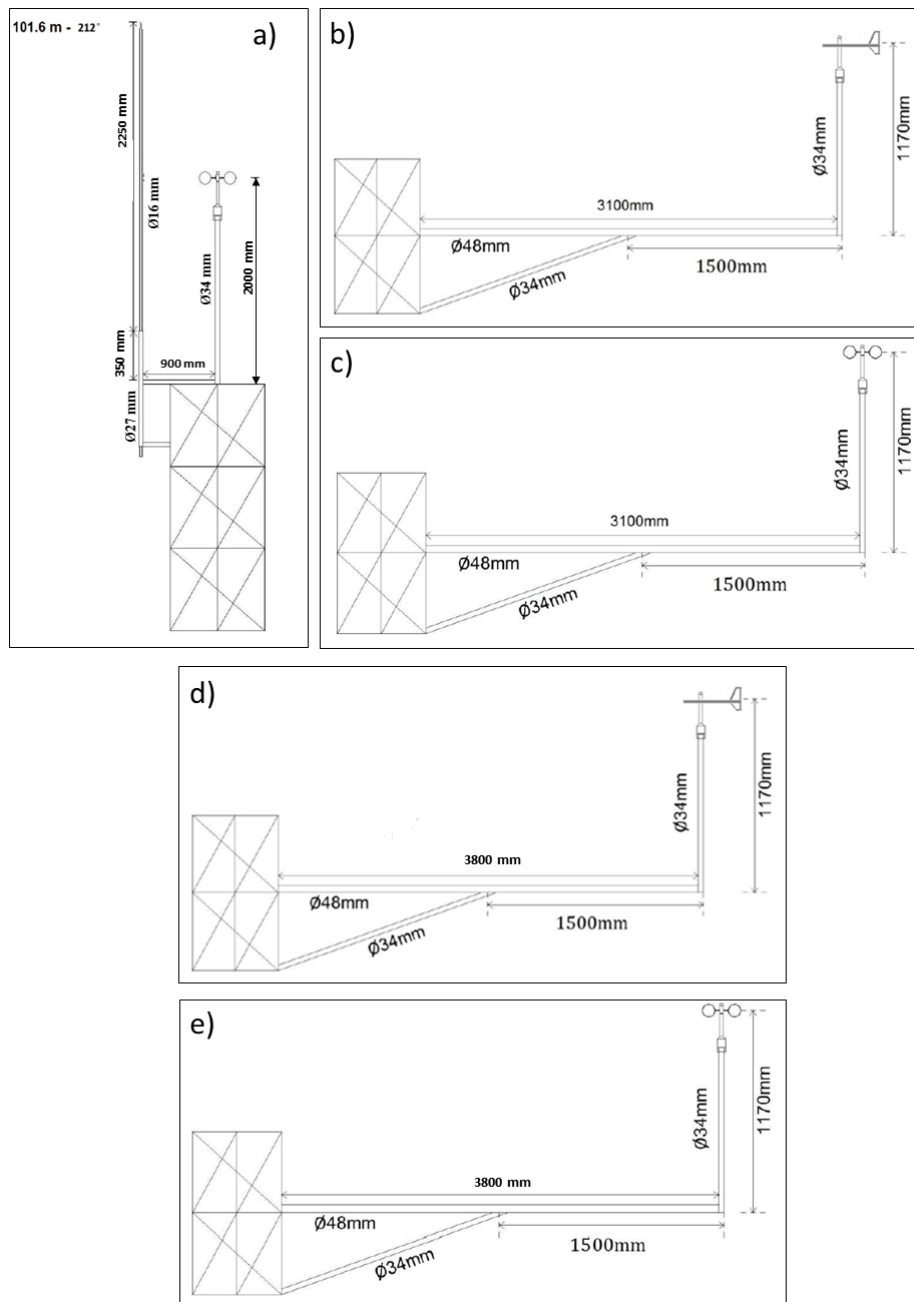


Figure 4.5. Technical drawing of the booms for the top and backup anemometers at 101 and 99 m, respectively, and wind vane at 98 m. Top anemometer, wind vane and backup anemometer are represented by a), b), and c), respectively.

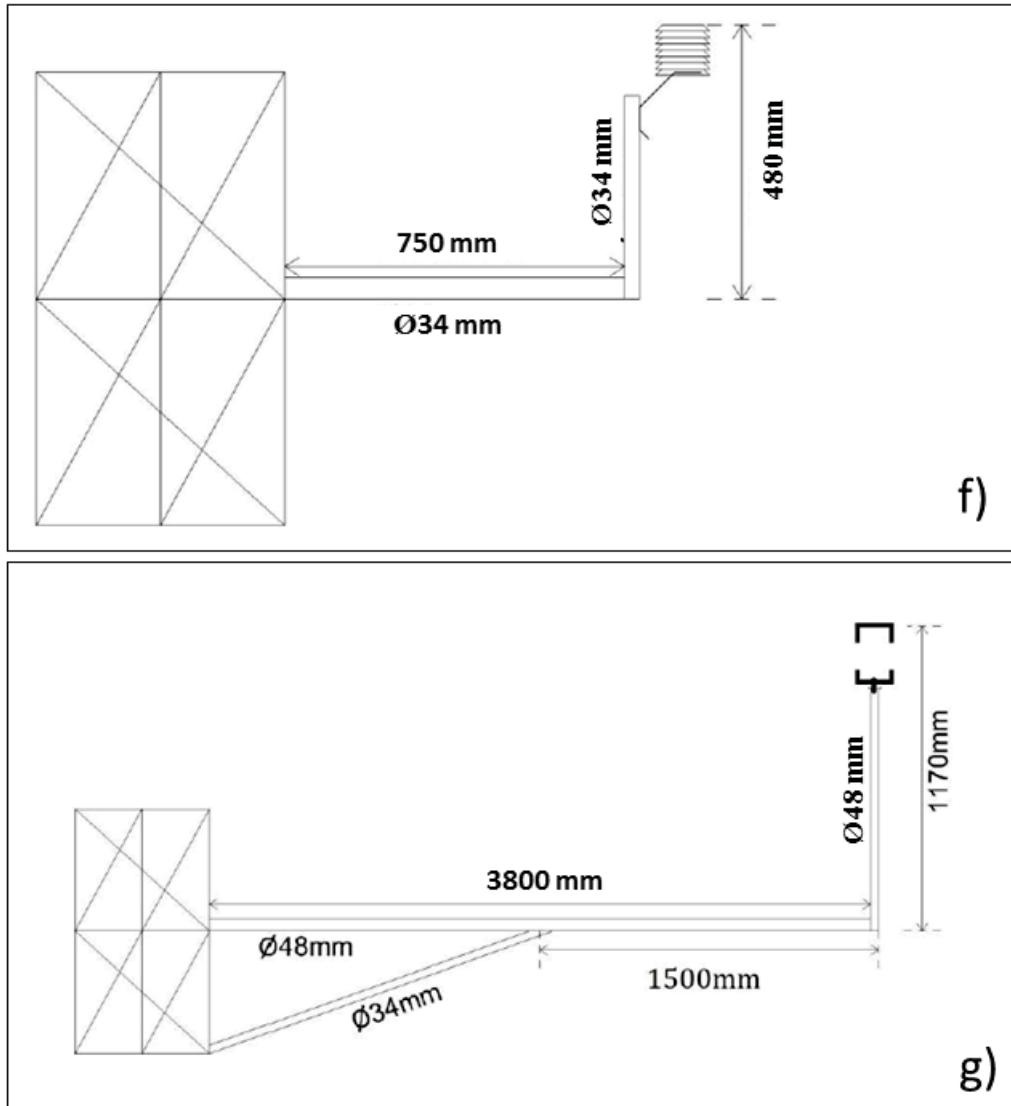


Figure 4.6. Technical drawing of the booms for the sonic anemometers and temperature/humidity sensors. Sonic anemometers mounted at 52 m and 10 m, while temperature/humidity sensors mounted at 3-35-90 m.

4.2. Measurement Campaign

IZTECH 100 m meteorological mast has been founded where the coordinates are N $38^{\circ}19'60''$ and E $26^{\circ}37'58''$ and the elevation from sea level is 52 m. The mast area can be shown in Figure 4.7. Here, the met mast area is very steeper and mountains also effects the wind flow where the wind flow comes.

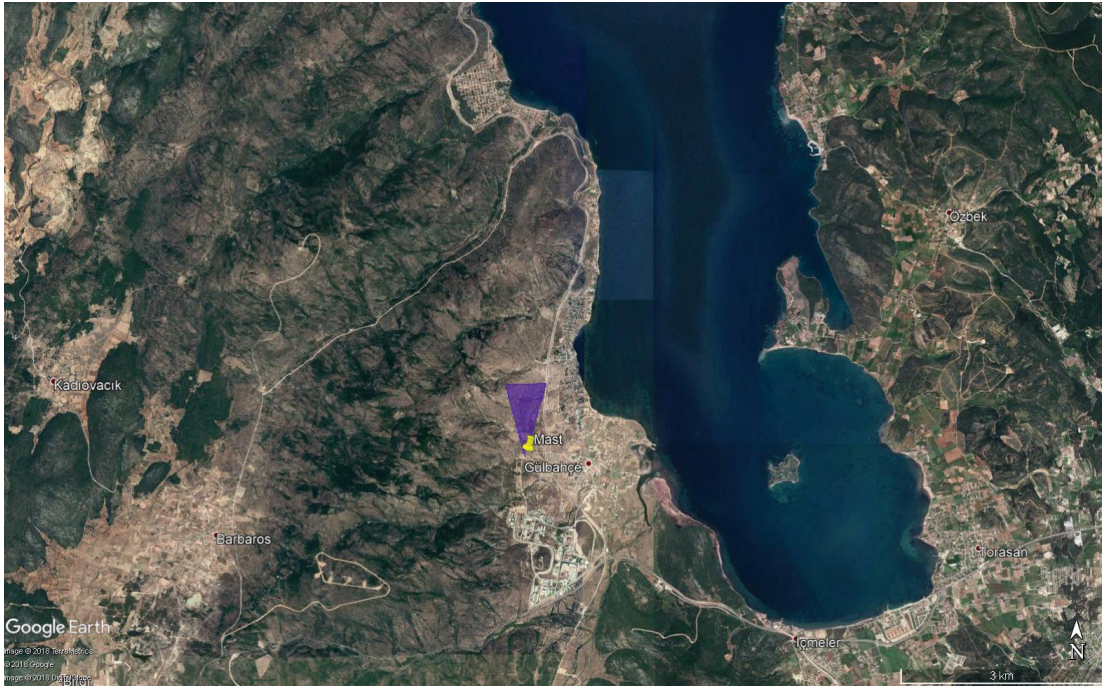


Figure 4.7. Location of the IZTECH met mast
(Source: Google Earth)

Measurements have been taken 6 months and data sampling rate is one second. Data samples are recorded as frequencies and they are needed to be rearranging with sensors coefficients. Parameters such as temperature, velocity, direction, and so on, from the sensors are not taken directly from the sensors since they are frequency samples.

In the Table 4.1 sensor locations, measured parameters, sensor types, and locations are given. All variables are grouped by measured parameters and their location or any other parameters investigated can be seen in the same column. There are also other values which can be derived by using parameters from channels above and one can see that what parameters are associated with derived values in Table 4.2.

In the Table 4.2, related parameters row shows that parameters are needed for obtaining derived ones e.g. to get the heat flux, horizontal and vertical velocity component

Table 4.1. IZTECH 100 m met mast properties

Height	Channel	Sensor	Unit
101.0m	WS_{101}	Thies First Class Adv. Anemometer	m/s
99.0m	WS_{99}		
76.0m	WS_{76}		
30.0m	WS_{30}		
52.0m	$WS_{52}, WD_{52}, \theta_{vir52}$	Gill WindMaster 3D Anemometer	$m/s, ^\circ, ^\circ C$
10.0m	$WS_{10}, WD_{10}, \theta_{vir10}$		
98.0m	WD_{98}	Thies First Class Wind Vane	°
74.0m	WD_{74}		
28.0m	WD_{28}		
90.0m	RH_{90}, T_{90}	Galtec KPC 1.S/6-ME	%, °C
35.0m	RH_{35}, T_{35}		
3.0m	RH_3, T_3		
90.0m	P_{90}	Thies 3.1157.10.000 Pressure	hPa
2.0m	P_2		
2 m	-	Ammonit Meteo40 Data Logger	-

Table 4.2. Derived parameters

Derived Values	Related Parameters
ρ_{10}	P_{10}, RH_{10}, T_{10}
ρ_{52}	P_{52}, RH_{52}, T_{52}
$u_{*,10}$	u_{10}, v_{10}, w_{10}
$u_{*,52}$	u_{52}, v_{52}, w_{52}
h_{Flux10}	$\rho_{10}, w_{10}, T_{10}$
h_{Flux52}	$\rho_{52}, w_{52}, T_{52}$
zL_{10}	w_{10}, T_{10}, u_{10}^*
zL_{52}	w_{52}, T_{52}, u_{52}^*

and density of the air are needed. After multiplication of the velocity components, time series of the temperature and the density which is also found by using the temperature, humidity, and pressure, heat flux can be obtained. Another point is subscripts which they point the location of the measurements. 10 represents the measurements taken from 10 m height by using sonic anemometer, while 52 represents the measurements taken from ultrasonic mounted on 52 m. All the parameters are taken from ultrasonic anemometers and they can be reached as 10 min averages in data logger both of the related parameters and derived values.

4.3. Data Analysis

In here the steps of the data processing is to be told which starts with the obtain of the raw data. Raw data need to be calibrated by using the gain and offset coefficients and data selection criteria which helps to get rid of unwanted data. Since measurements are taken from discrete points, interpolation can be used for determining any point in this range. In this study Lagrange interpolation used owing to it gives more accurate results where the measurements are taken from 3 different altitudes. Thanks to wind measurements, dimensionless wind shear can be estimated by using fitting 2nd order polynomial in $\ln(z)$, defined as

$$U(z) = U_0 + U_1 \ln(z) + U_2 [\ln(z)]^2 \quad (4.1)$$

$$\phi_m = \frac{\kappa}{u_{*0}} [U_1 + 2U_2 \ln(z)]$$

where z is the height of the measurement point and U_0, U_1 , and U_2 coefficients are to find by using least square method. Furthermore, data selection criteria is used to filter sensor error and signal noises those are:

- Wind speeds less than 1 m/s are excluded ,
- Wind direction from $[345^\circ, 15^\circ]$,
- surface roughness bigger than 1 m is excluded.
- ζ is chosen from $[-2, 2]$,
- $|T_*| > 0.05^\circ\text{C}$ (Dellwik and Jensen, 2005),
- $|H| \geq 10 \text{ W m}^{-2}$ and $u_{*0} \geq 0.1 \text{ W m}^{-1}$ to estimate ϕ_h (Högström, 1988),
- $u_{*0} \geq 0.1 \text{ W m}^{-1}$ in order to determine ϕ_m (Högström, 1988).

When there is a time series calibrated then averaging comes next. Averaging part is very important since all the effect of turbulence may not be seen after averaging whether it is close to gap scale of the turbulence or not, and then only mesoscale effects are going to be seen.

Averaged values are used to find fluctuations which helps to find flux values. The difference between mean value and value at a certain time in time series gives the fluctuation. Wind speed, humidity, temperature, and direction are used to find scalar and

vectorial flux such as heat and momentum fluxes, respectively. In processing virtual potential temperature sonic temperature is used directly since the sonic anemometers are measures independent from the humidity which result in higher temperature measurements almost equal to virtual potential temperature as in (Schotanus et al., 1983) and (Kaimal and Gaynor, 1991).

Next is to derive values that is used for obtaining Obukhov length, friction velocity, and temperature scales then classification can be easily done depending on the Obukhov length.

4.3.1. Flux-Profile Relation

Flux relations in the surface layer and in the other layers such as ML, z-Less stratification, and etc. are given earlier and some dimensionless parameters derived by using them which called as profile parameters. In this part aim is to give relations between flux and profile parameters which they are obtained by using the least squares method by many authors such as Businger et al, 1971; Dyer,1974; Dyer and Bradley, 1982; Zilitinkevich and Chalikov, 1968; Foken and Skeib, 1983; Swinbank, 1964-1968; Webb, 1970; Panofsky, 1960 and so on.

Their works basically related with putting an empirical relation between dimensionless Obukhov Length and profile parameters depending on the class of stability. For this reason many experiments have been performed by authors.

Businger et al.,1971, have shown that for both of the stable and unstable situations velocity and heat profile are given but those are valid under the $\zeta \geq -2$ and on the wheat farm surface or any surface resembles to wheat farm. F-P relations by Businger et al. given at Table 4.3.

Table 4.3. F-P Relationships for instability cases by Businger et al.

Case/ κ	Unstable	Stable
$\kappa = 0.35$	$\phi_m = (1 - 15\zeta)^{-1/4}$ $\phi_h = (1 - 9\zeta)^{-1/2}$	$\phi_m = 1 + 4.7\zeta$ $\phi_h = 0.74 + 4.7\zeta$
$\kappa = 0.40$	$\phi_m = (1 - 19.3\zeta)^{-1/4}$ $\phi_h = 0.95 (1 - 11.6\zeta)^{-1/2}$	$\phi_m = 1 + 6\zeta$ $\phi_h = 0.95 + 7.8\zeta$

Dyer's results work well on the conditions such as roughness similar to ocean's surface and the range of dimensionless stability parameter is between $[-1, 0]$.

Table 4.4. F-P Relationships for instability cases by Dyer

Case/ κ	Unstable	Stable
$\kappa = 0.41$	$\phi_m = (1 - 16\zeta)^{-1/4}$ $\phi_h = (1 - 16\zeta)^{-1/2}$	$\phi_m = 1 + 4.7\zeta$ $\phi_h = 1 + 5\zeta$
$\kappa = 0.40$	$\phi_m = (1 - 15.2\zeta)^{-1/4}$ $\phi_h = 0.95(1 - 15.2\zeta)^{-1/2}$	$\phi_m = 1 + 6\zeta$ $\phi_h = 0.95 + 4.5\zeta$

In Dyer and Bradley's approach surface roughness has taken for grass-field and there is an expression only for unstable situation which is $\phi_m = (1 - 28\zeta)^{-1/4}$ where $\kappa = 0.40$

In Zilitinkevich and Chalikov, 1968, limits of the stability range is given between of the $[-0.16, 0]$ this shows that equation works well in this range and for grass fields, while out of this range it diverges from real situation. Their result is:

Table 4.5. F-P Relationships for instability cases by Zilitinkevich and Chalikov

Case/ κ	Unstable	Stable
$\kappa = 0.43$	$\phi_m = 1 + 1.45\zeta$ $\phi_h = 1 + 1.45\zeta$	$\phi_m = 1 + 9.9\zeta$ $\phi_h = 1 + 9.9\zeta$
$\kappa = 0.40$	$\phi_m = 1 + 1.38\zeta$ $\phi_h = 0.95 - 1.31\zeta$	$\phi_m = 1 + 6\zeta$ $\phi_h = 0.95 + 8.9\zeta$

For extreme conditions they found that those linear relations change and form as $\phi_m = 0.4(-\zeta)^{-1/3}$ and $\phi_h = 0.4(-\zeta)^{-1/3}$. It can be seen that under unstable condition for both velocity and temperature profiles are 3rd order relations while they are linear under stable conditions.

Diabatic term (non-neutral stratification) is obtained by the integration of profile expressions as given Equation 3.39 which has derived by using Businger - Dyer relations. Finally wind velocity equation is rearranged:

$$u(z) = \frac{u_*}{\kappa} \left[\ln \left(\frac{z}{z_0} \right) + 4.7\zeta \right] \quad (4.2)$$

$$u(z) = \frac{u_*}{\kappa} \left[\ln \left(\frac{z}{z_0} \right) - 2 \ln \left[\frac{(1+x)}{2} \right] - \ln \left[\frac{(1+x^2)}{2} \right] + 2 \arctan x - \frac{\pi}{2} \right] \quad (4.3)$$

where $x = (1 - 15\zeta)^{0.25}$

4.3.2. Richardson Method

Richardson number is a relation between buoyant forces and wind shear gradient which gives idea of the existence of turbulence. In additionally it is related with the stability term ζ where it can also be used for regarding the instability.

There are several type of approaches for this method and first one flux Richardson method which is given as:

$$R_f = \frac{\left(\frac{g}{\theta_v}\right) (\overline{w'\theta'_v})}{(\overline{u'_i u'_j}) \frac{\partial \overline{U}_i}{\partial x_j}} \quad (4.4)$$

When unstable flow occurs it can be seen that R_f becomes negative, for neutral condition it goes to 0, for stable situations it becomes positive, and when the mechanical forces are balanced with the thermals which called as critical condition. Considering the last claim when;

$$R_f < 1 : \text{Turbulent Flow}$$

$$R_f > 1 : \text{tends to become Laminar Flow}$$

The restrictions for this method is that giving idea only if turbulence will be exist or not, however any idea regarding the future of laminar flow can not be obtained. To solve this problem gradient Richardson method derived by using K-theory where lapse rate and velocity gradients used instead of fluxes in Equation 4.4

$$Ri = \frac{\frac{g}{\theta_v} \frac{\partial \overline{\theta}_v}{\partial z}}{\left(\frac{\partial \overline{u}}{\partial z}\right)^2 + \left(\frac{\partial \overline{v}}{\partial z}\right)^2} \quad (4.5)$$

As another consideration between Ri and R_f has done as:

$$Ri < R_c : \text{Laminar} \rightarrow \text{Turbulence}$$

$$Ri > R_T : \text{Turbulence} \rightarrow \text{Laminar}$$

where R_T mention to expiration of the turbulence.

Lastly, Bulk Richardson method has derived which regards discrete height and makes calculations simpler comparing to previous methods. In order to calculate different 2 heights are needed which is:

$$Ri_B = \frac{g \Delta \overline{\theta}_v \Delta z}{\overline{\theta}_v [(\Delta \overline{u})^2 + (\Delta \overline{v})^2]} \quad (4.6)$$

when the one of the height is taken at surface roughness velocity becomes 0 and that makes this method very charming to choose. Another advantage of this method is that in meteorology measurements are taken at discrete points of heights. When the difference between two discrete points large enough critical points diverge from the given values.

The link between Ri_B and Obukhov Length is expressed as,

$$\frac{z}{L} = C_1 Ri_B \quad (4.7)$$

$$\frac{z}{L} = \frac{C_1 Ri_B}{1 - C_2 Ri_B} \quad (4.8)$$

In literature many works done to obtain those C_1 and C_2 coefficients and some results are; $C_1 = 10$ for Equation 4.7 where $-1 < Ri_B < 0$ and $C_1 = 10, C_2 = 5$ for Equation 4.8 for unstable and stable cases offered by , respectively. Deardorff, 1968 is estimated C_1 as 12 in between -0.012 and 0.012. In a different study this number calculated between 6.78 for the conditions when the $-20 < U\Delta\Theta < 20$. On the other hand it is 10.89 when $U\Delta\Theta > 20$. As it can be seen under this circumstances critical Richardson value is obtained as 0.2 (Grachev and Fairall, 1996). These are some restrictions and the relation between Richardson number and Obukhov Legth is very basic in perspective of given only stable and unstable stability class.

4.3.3. Wind Shear Exponent

As an another method wind shear exponent by Elliott et all. (1987) can be used for obtaining vertical wind profile and defined as:

$$U(z_2) = U(z_1) \left(\frac{z_2}{z_1} \right)^\alpha \quad (4.9)$$

Wind shear exponent varies with air stability and surface roughness (Blackadar, 1997). So in complex or heterogeneous terrain z_0 changes a lot with wind direction or better to say that in every sector different scenario can be seen. It expressed as function of dimensionless wind velocity parameter and roughness length in Equation 4.10, (Blackadar, 1997):

$$\alpha = \frac{\phi_m \left(\frac{z}{L} \right)}{\ln \left(\frac{z}{z_0} \right) - \psi_m \left(\frac{z}{L} \right)} \quad (4.10)$$

When one looks at the wind shear exponent it can be realized that under strong(pure) stable case wind shear highest and wind velocity is high, very unstable(convective) conditions negative values seem and horizontal speed is lowest respect to other cases. The strongest wind velocity occurs in near neutral condition.

Table 4.6. Stability classes with shear exponent
(Source:Van den Berg 2008)

Pasquill class	Name	Shear exponent range	Shear exponent value
A-C	(Very-Slightly) Unstable	$m \leq 0.1$	0.07-0.1
D	(Near) Neutral	$0.1 < m \leq 0.2$	0.15
E	Slightly Unstable	$0.2 < m \leq 0.4$	0.35
F	(Moderately-very) Stable	$0.4 \leq m$	0.55

In Table 4.6, Pasquill classification system has been given with shear exponents. In that work wind shear exponent ranges and real values belonged to that work given, too. It can be seen that m number gets bigger when the stable stratification occurs and it approaches to 1/7 which used generally in calculations.

This method doesn't give the stability directly, however it gives idea the range of stability which makes it useful. After finding shear range of the stability can be found from the Table 4.6. Then a comparison between the stability classes found by shear method and MOST is possible.

CHAPTER 5

RESULTS

In this chapter, firstly the theory known as Richardson which gives opportunity to derive Obukhov length by using flux profile relations is given. The physical relation isn't easy to solve for unstable conditions now that equation becomes non-linear. However for stable conditions where it starts to pass local z-less stratification its characteristics become more linear. Derived Obukhov length and MOST-based one are compared.

Secondly, wind shear parameter and how they interact with the stability class will be given. A comparison between the number of the obtained classes by wind shear exponent and MOST are going to be shown.

At last, wind speed averages at 2 heights; 10 m and 52 m, and averages of measured velocities are shown where the velocities are averaged depending on the stability classes.

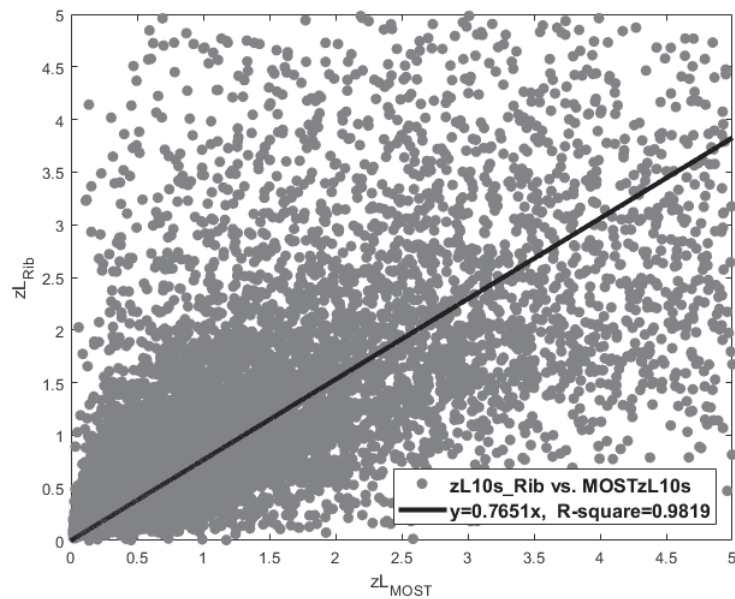


Figure 5.1. Dimensionless Obukhov length parameters for the stable region at 10 m

In Figure 5.1, it can be seen that data gather around near the 0, since the region is near neutral conditions. As it gets closer to 0 linear approaches becomes more suitable,

on the contrary, it doesn't work after 2 due to the existence of strongly stable conditions.

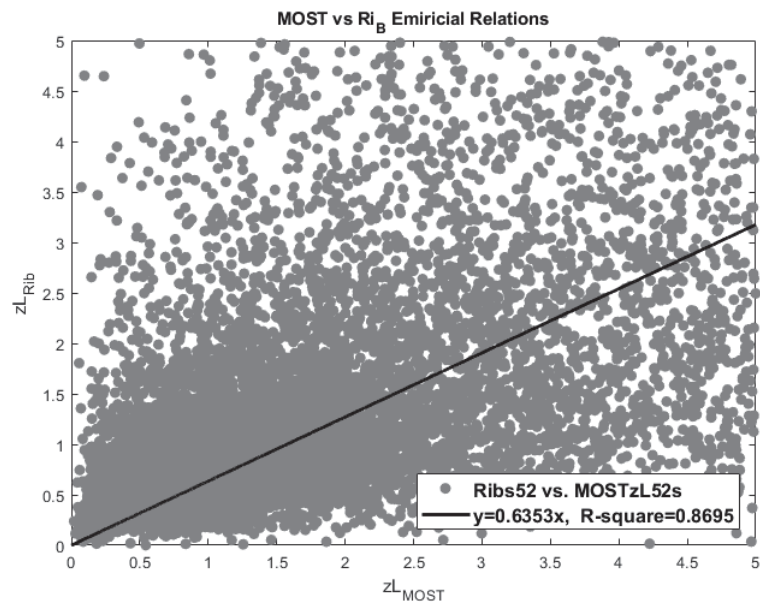


Figure 5.2. Dimensionless Obukhov length parameters for the stable region at 52 m

In Figure 5.2 it can be realized that data are much more scattered respect to Figure 5.1 since the theory of Richardson number is valid under the turbulence. When mesoscale effects are dominant, the applicability of the Rib is gets weaker. So, on the surface it is known that friction forces are affective which is the reason of turbulence and far from the source it gets weaker and it dies in the end.

For unstable region bias and scatter is higher and it is realized that z/L depending on the Richardson number gives underestimated results. Most of the data placed at the left side of the diagonal. Since unstable region is non-linear, being very hard to obtain cause it is complex terrain, and lastly kinematic heat fluxes estimated by the help of vertical velocity component makes very hard to use Richardson for unstable region which can be seen in Figure 5.4.

That is unexpected result that scattering is more even than the Figure 5.3. Underestimation of the z/L gets faint since the wind shear gets weaker and vertical motion of air becomes stronger. Fitted function derived by using least absolute residuals method in MATLAB instead of least error square (LES). Here R-square is very close to 1, however, many data point is missing due to the lack of the quality of the Richardson approaches. Therefore, Richardson approaches don't work well for the unstable conditions.

Richardson method works well for the stable conditions in a limited region and

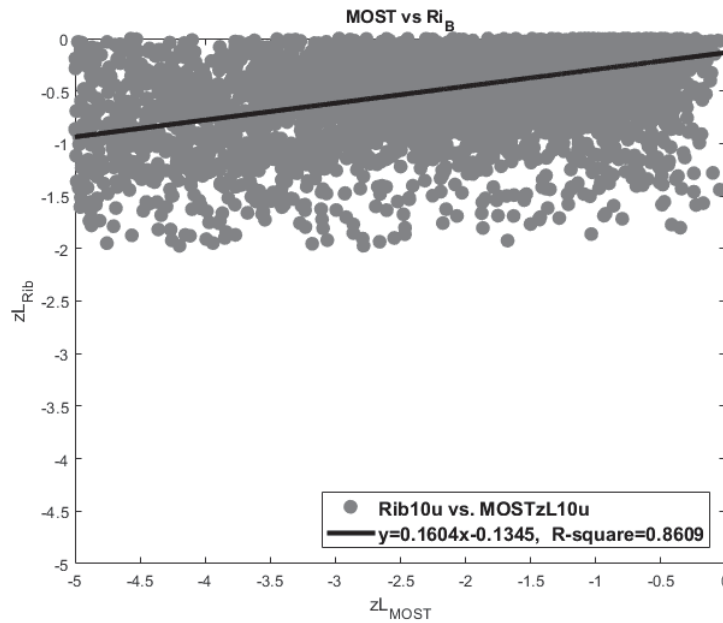


Figure 5.3. Dimensionless Obukhov length parameters for the unstable region at 10 m

for extreme conditions it is not useful. Another suggested approach is the wind shear exponent which is studied by many authors (DeMarrais, 1959), (Touma, 1977), (Sutton, 1947), and (Heald and Mahrt, 1981).

By using the values from table 4.6 and using the stability range criteria a comparison between stability classes where one of them obtained by using MOST and other one by using wind shear exponent.

It seems that under neutral condition both methods give very good results, on the contrary under the strongly convective and stable conditions the results obtained by the wind shear exponents diverge from the MOST.

Lastly wind velocities are from different classes such as unstable, stable, neutral, and all of them together will be shown with the logarithmic wind profile which is fitted by using the average friction velocity at the surface and κ as 0.41 and average of roughness from the neutral region. Since only having 2 ultrasonic anemometer results are not enough but anyway the underestimation and overestimation of the wind velocities can be seen from Figure 5.6.

From the Figure 5.6 seems that wind velocity calculated by using all the data and averaged velocities at that location differ from each other. When the case is unstable then averaged velocity smaller than what is expected near the ground. In fact, it is same for all

the cases and it shows that using all data give result to overestimate near the ground. At 52 m it seems that all cases get along well out of the neutral cases.

As it can be seen from Figure 5.7, wind shear is maximum under neutral conditions and minimum when all data are used. In normalized plot the importance of the stability analysis can be seen. When the data used in wind flow models, neutral velocity should be used to prevent biased results.

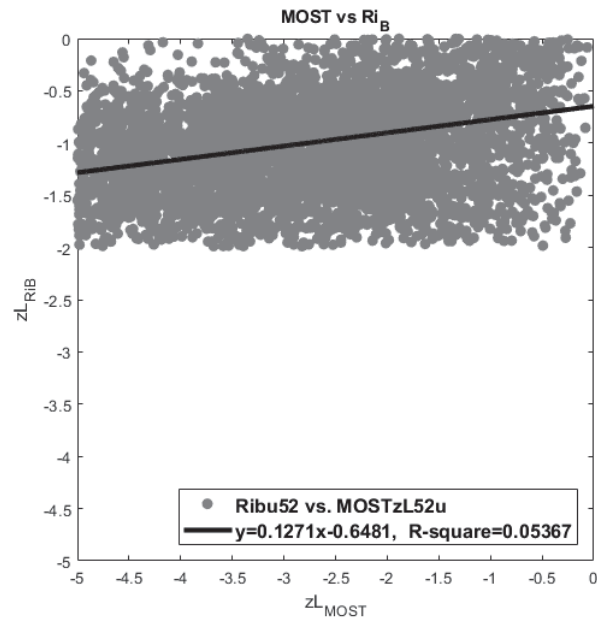


Figure 5.4. Dimensionless Obukhov length parameters for the unstable region at 52 m

Even for unstable and stable conditions get along well with the all data far from the ground, the reason is 90% of the data belongs to instability region and only 10% of data is neutral. Therefore the difference comes from that case. Near the ground it can be easily see that there are big difference on the averages since friction effects get higher.

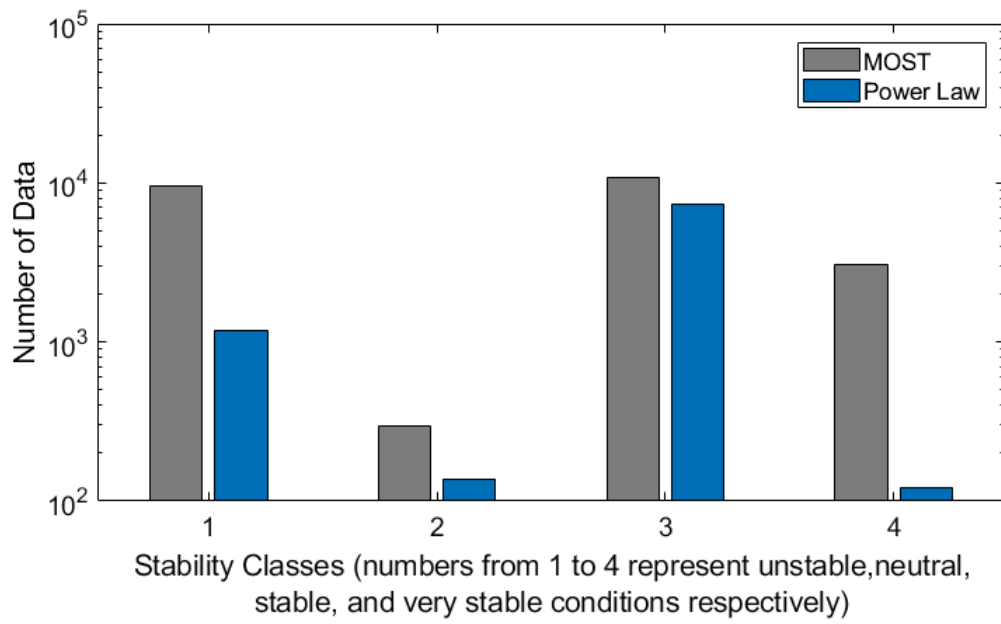


Figure 5.5. Comparison of stability classes by MOST and wind shear exponent

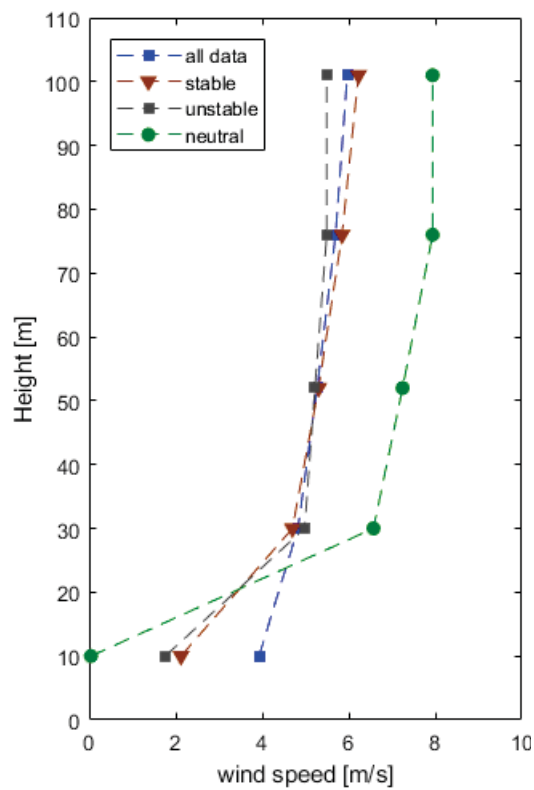


Figure 5.6. Wind velocities at different heights from met mast

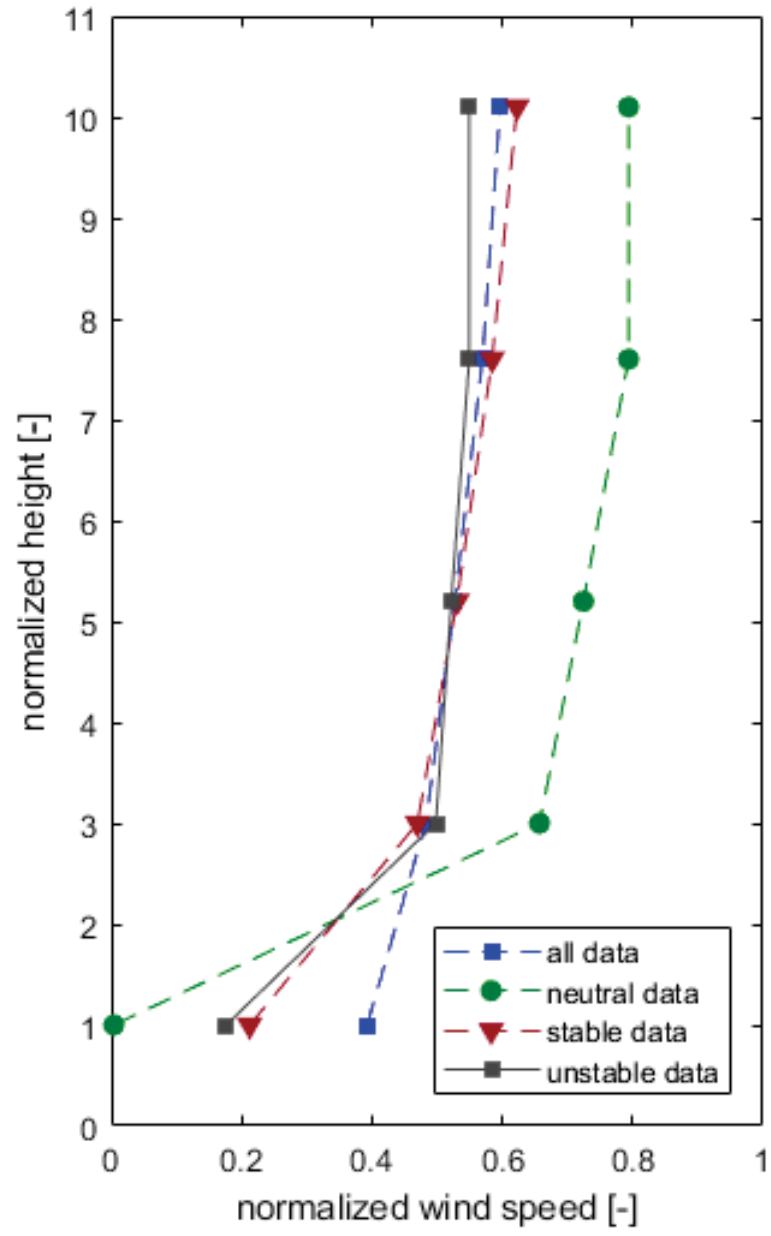


Figure 5.7. Normalized wind velocity versus height graph

CHAPTER 6

DISCUSSION

Considering the instability, surface characteristics, and measurement those are taken several different points which checked cautiously this study is very comprehensive and can be used for different kind of events such as different surfaces, seasons, altitudes, and so on. The reason behind for last statement that in this work ultrasonic measurement devices used at 2 discrete points. Pressure, humidity, temperature, direction, and velocity samples ratio is 1 Hz, several different gap scale performed for the timescale domain in order to get rid of mesoscale effects since all theories told before regard turbulent flow.

In Turkey, several thousands of meteorological mast exist where temperature, humidity, and vertical heat fluxes are ignored and those masts are insufficient in terms of giving idea about structure of the vertical ABL since they are up to 80 m. On the other hand IZTECH met-mast is 100 m and 2 ultrasonic anemometer used where one of them mounted on the 10 m and other one placed at 52 m. Sonic anemometer at 10 m is useful for investigating surface characteristics and other one which is at 52 m is beneficial for obtaining the structure of ABL above the surface layer where local fluxes are effective and large eddies can be seen. Another deficiency in wind energy researches is that having time series to make an analyses where in many study only averaged values are used and sometimes bias can be extreme.

The response time of the sonic anemometers are not enough to make a turbulence analyses since 1 Hz is not enough to observe small eddies and in order to achieve this problem ultrasonic anemometers where the response time is shorter can be used as a future work. Data from lidar, sodar, and sonic can be benchmarked to see bias on measurements and derived values such as ζ , Ri , R_f , and so on. Since there is no mobility problem in Sodar and Lidar, more comprehensive wind measurements can be performed on the complex terrain by changing location of them.

CHAPTER 7

CONCLUSION

In this study many approaches have been compared and it has found that MOST is valid for SL as it is proposed, Richardson similarity theory is not working well since the are is not flat, however if this approach modified it seems that better results can be obtained. MOST analyses is easy to perform by using the sonic anemometers since momentum fluxes which those are used to obtain friction velocity can measured. On the contrary it is complex for conventional system since there isn't an option as previous one. Nevertheless, it observed Richardson, wind shear, and F-P profile relations are valid in specified regions and for extreme instability conditions extra cautious is needed for considering the results.

The time scale is important parameter to consider since it can be inferred from the results that when different gap scale are used to perform similarity theories and stability analyses it seems that bias changes, too. In order to do better analyse on stability surface roughness, temperature gradient, and time gap should be chosen cautiously.

F-P relations are not in good agreement with the literature but the reason behind that those experiments are performed for flat terrain and time series are much longer respect to this work. Another reason is that those relations are empirical so depending on the surface characteristics it is normal to expect this conclusion.

Wind shear method is provides a wide range of usage since depended only height and shear exponent. However it is obvious that wind shear exponent also depends stability parameter and another problem is wind shear exponent can differ according to wind direction.

Finally, in wind velocity and temperature estimation it is very crucial that to use all time series is worst option and the appropriate one is either to choose only neutral condition or to use necessary calculation in order to get ψ term and rearrange equations.

REFERENCES

- Arnqvist, J., A. Segalini, E. Dellwik, and H. Bergström (2015). Wind statistics from a forested landscape. *Boundary-Layer Meteorology* 156(1), 53–71.
- Arya, S. (1984). Parametric relations for the atmospheric boundary layer. *Boundary-Layer Meteorology* 30(1-4), 57–73.
- Blackadar, A. K. (1962). The vertical distribution of wind and turbulent exchange in a neutral atmosphere. *Journal of Geophysical Research* 67(8), 3095–3102.
- Burns, S., T. Horst, L. Jacobsen, P. Blanken, and R. Monson (2012). Using sonic anemometer temperature to measure sensible heat flux in strong winds. *Atmospheric Measurement Techniques* 5(9), 2095–2111.
- Businger, J. A., J. C. Wyngaard, Y. Izumi, and E. F. Bradley (1971). Flux-profile relationships in the atmospheric surface layer. *Journal of the Atmospheric Sciences* 28(2), 181–189.
- Byun, D. W. (1990). On the analytical solutions of flux-profile relationships for the atmospheric surface layer. *Journal of Applied Meteorology* 29(7), 652–657.
- Dellwik, E. and N. O. Jensen (2005). Flux–profile relationships over a fetch limited beech forest. *Boundary-layer meteorology* 115(2), 179.
- DeMarrais, G. A. (1959). Wind-speed profiles at brookhaven national laboratory. *Journal of Meteorology* 16(2), 181–190.
- Dias, N., J. Gonçalves, L. Freire, T. Hasegawa, and A. Malheiros (2012). Obtaining potential virtual temperature profiles, entrainment fluxes, and spectra from mini unmanned aerial vehicle data. *Boundary-layer meteorology* 145(1), 93–111.
- Dyer, A. (1974). A review of flux-profile relationships. *Boundary-Layer Meteorology* 7(3), 363–372.
- Dyer, A. and B. Hicks (1970). Flux-gradient relationships in the constant flux layer. *Quarterly Journal of the Royal Meteorological Society* 96(410), 715–721.
- Ellison, T. (1957). Turbulent transport of heat and momentum from an infinite rough plane. *Journal of Fluid Mechanics* 2(5), 456–466.
- Floors, R., C. L. Vincent, S.-E. Gryning, A. Peña, and E. Batchvarova (2013). The wind profile in the coastal boundary layer: Wind lidar measurements and numerical modelling. *Boundary-layer meteorology* 147(3), 469–491.
- Foken, T. and G. Skeib (1983). Profile measurements in the atmospheric near-surface layer and the use of suitable universal functions for the determination of the turbulent

- energy exchange. *Boundary-Layer Meteorology* 25(1), 55–62.
- Golder, D. (1972). Relations among stability parameters in the surface layer. *Boundary-Layer Meteorology* 3(1), 47–58.
- Grachev, A., C. Fairall, and E. Bradley (2000). Convective profile constants revisited. *Boundary-layer meteorology* 94(3), 495–515.
- Grachev, A. A., E. L. Andreas, C. W. Fairall, P. S. Guest, and P. O. G. Persson (2007). Sheba flux–profile relationships in the stable atmospheric boundary layer. *Boundary-layer meteorology* 124(3), 315–333.
- Grachev, A. A., E. L. Andreas, C. W. Fairall, P. S. Guest, and P. O. G. Persson (2013). The critical richardson number and limits of applicability of local similarity theory in the stable boundary layer. *Boundary-layer meteorology* 147(1), 51–82.
- Gryning, S.-E., E. Batchvarova, B. Brümmner, H. Jørgensen, and S. Larsen (2007). On the extension of the wind profile over homogeneous terrain beyond the surface boundary layer. *Boundary-Layer Meteorology* 124(2), 251–268.
- Halstead, M. (1943). A stability-term in the wind-gradient equation. *Eos, Transactions American Geophysical Union* 24(1), 204–208.
- Heald, R. and L. Mahrt (1981). The dependence of boundary-layer shear on diurnal variation of stability. *Journal of Applied Meteorology* 20(8), 859–867.
- Högström, U. (1988). Non-dimensional wind and temperature profiles in the atmospheric surface layer: A re-evaluation. In *Topics in Micrometeorology. A Festschrift for Arch Dyer*, pp. 55–78. Springer.
- Holzman, B. (1943). The influence of stability on evaporation. *Annals of the New York Academy of Sciences* 44(1), 13–18.
- Jiménez, P. A., J. Dudhia, J. F. González-Rouco, J. Navarro, J. P. Montávez, and E. García-Bustamante (2012). A revised scheme for the wrf surface layer formulation. *Monthly Weather Review* 140(3), 898–918.
- Kaimal, J. and J. Gaynor (1991). Another look at sonic thermometry. *Boundary-Layer Meteorology* 56(4), 401–410.
- Kaimal, J. C. and J. J. Finnigan (1994). *Atmospheric boundary layer flows: their structure and measurement*. Oxford university press.
- Kot, S. C. and Y. Song (1998). An improvement of the louis scheme for the surface layer in an atmospheric modelling system. *Boundary-layer meteorology* 88(2).
- Landberg, L. (2015). *Meteorology for wind energy: an introduction*. John Wiley & Sons.

- Lettau, H. (1950). A re-examination of the “leipzig wind profile” considering some relations between wind and turbulence in the frictional layer. *Tellus* 2(2), 125–129.
- Monin, A. and A. Obukhov (1954). Basic laws of turbulent mixing in the surface layer of the atmosphere. *Contrib. Geophys. Inst. Acad. Sci. USSR* 151(163), e187.
- Panofsky, H., A. Blackadar, and G. McVehil (1960). The diabatic wind profile. *Quarterly Journal of the Royal Meteorological Society* 86(369), 390–398.
- Panofsky, H., D. Larko, R. Lipschutz, G. Stone, E. Bradley, A. J. Bowen, and J. Højstrup (1982). Spectra of velocity components over complex terrain. *Quarterly Journal of the Royal Meteorological Society* 108(455), 215–230.
- Peña, A. and A. N. Hahmann (2012). Atmospheric stability and turbulence fluxes at horns rev—an intercomparison of sonic, bulk and wrf model data. *Wind Energy* 15(5), 717–731.
- Prandtl, L. (1925). Bericht über untersuchungen zur ausgebildeten turbulenz. *Zs. angew. Math. Mech.* 5, 136–139.
- Reynolds, O. (1883). Xxix. an experimental investigation of the circumstances which determine whether the motion of water shall be direct or sinuous, and of the law of resistance in parallel channels. *Philosophical Transactions of the Royal Society of London* 174, 935–982.
- Schotanus, P., F. Nieuwstadt, and H. De Bruin (1983). Temperature measurement with a sonic anemometer and its application to heat and moisture fluxes. *Boundary-Layer Meteorology* 26(1), 81–93.
- Sorbjan, Z. and A. A. Grachev (2010). An evaluation of the flux–gradient relationship in the stable boundary layer. *Boundary-layer meteorology* 135(3), 385–405.
- Stull, R. B. (2012). *An introduction to boundary layer meteorology*, Volume 13. Springer Science & Business Media.
- Sutton, O. (1947). The problem of diffusion in the lower atmosphere. *Quarterly Journal of the Royal Meteorological Society* 73(317-318), 257–281.
- Sutton, O. G. (1932). A theory of eddy diffusion in the atmosphere. *Proc. R. Soc. Lond. A* 135(826), 143–165.
- Taylor, G. I. (1935). Statistical theory of turbulence. *Proceedings of the Royal Society of London. Series A, Mathematical and Physical Sciences* 151(873), 421–444.
- Taylor, G. I. (1938). The spectrum of turbulence. *Proceedings of the Royal Society of London. Series A, Mathematical and Physical Sciences*, 476–490.
- Tennekes, H. (1984). Similarity relations, scaling laws and spectral dynamics. In *Atmospheric turbulence and air pollution modelling*, pp. 37–68. Springer.

- Touma, J. S. (1977). Dependence of the wind profile power law on stability for various locations. *Journal of the Air Pollution Control Association* 27(9), 863–866.
- Van den Berg, G. (2008). Wind turbine power and sound in relation to atmospheric stability. *Wind Energy* 11(2), 151–169.
- Wyngaard, J., O. Coté, and Y. Izumi (1971). Local free convection, similarity, and the budgets of shear stress and heat flux. *Journal of the Atmospheric Sciences* 28(7), 1171–1182.
- Yang, K., N. Tamai, and T. Koike (2001). Analytical solution of surface layer similarity equations. *Journal of Applied Meteorology* 40(9), 1647–1653.